Cantilever interaction of shear walls and frames

CANTILEVER INTERACTION OF SHEAR WALLS AND FRAMES

by

Chimanbhai N. Patel

A Thesis Submitted to the Faculty of the

DEPARTMENT OF CIVIL ENGINEERING

In Partial Fulfillment of the Requirements
For the Degree of

MASTER OF SCIENCE

In the Graduate College

THE UNIVERSITY OF ARIZONA

1 9 6 8

STATEMENT BY AUTHOR

SIGNED: Chimanbhai N. Patel

APPROVAL BY THESIS DIRECTOR

This thesis has been approved on the date shown below:

Andrew W. Ross — Nov. 16, 1967

Andrew W. Ross
Professor of Civil Engineering

Date

ACKNOWLEDGMENT

The author wishes to express his deep gratitude to his thesis director, Professor Andrew W. Ross, for his active interest, helpful guidance and constructive suggestions.

He would also like to express his appreciation to Rod Gomez and Assoc., Consulting Engineers, Tucson, Arizona., for the practical training he received.

TABLE OF CONTENTS

Table of Contents (Continued)

LIST OF ILLUSTRATIONS

LIST OF TABLES

ABSTRACT

If a building consisting of frames and shear walls is replaced by two representative cantilevers; then one cantilever represents the frame and the other the shear wall or assembly of shear walls. In the analysis of the interaction of the shear wall and frames, use of this concept of twin cantilevers is made in order to save a considerable amount of manual work in moment distribution.

For an approximate deflected shape of the frame, the developed forces and moments are calculated at the joint between shear wall and frame at each story. The balance of forces and moments (loading and frame) are applied to the shear wall to find the deflection of the wall at each story. This iterative procedure is carried on until the following conditions are satisfied.

That; the horizontal deflection must be the same in both cantilevers at corresponding levels.

That; the summation of shears developed in both cantilevers must be equal to the total external shear (due to loading) at every story.

Effects of base rotation of the shear wall are included also in the analysis.

This thesis is an attempt to both simplify and abbreviate existing techniques for accomplishing the above by combining methods suggested in recent literature.

CHAPTER 1

INTRODUCTION

As multistory building construction has evolved from bearing wall types of the late 19th century and the rigid steel frames of the 1930's to the delicate curtain wall buildings of the 1950's, the interior compositions have changed along with the exterior skins (3). The trends toward column-free interiors, long spans, minimum floor to floor heights and maximum rentable area together with the increased popularity of reinforced concrete as a construction material have resulted in the use of the shear wall as the principal lateral load resisting member in many multistory buildings. Frequently the service core of the building has provided an excellent location for the shear wall since enclosure walls are required there anyhow.

Since a large number of tall buildings are now being constructed, and present practice in this type of construction is to provide shear walls along with the frames to resist lateral loads due to wind or earthquake, the design of shear walls has been the subject of considerable discussion in the past few years.

The simplest approach to the design problem is to consider the shear wall as an independent member and design it as a vertical cantilever. But since the steel framing actually does resist some of the lateral loading, such design is quite conservative with respect to shear walls; whereas the frames are underdesigned.

A number of excellent articles have been published on the subject of interaction of shear walls with frames in multistory structures (2,3,4,5). The analyses presented in the aforementioned papers are, of course, interesting and applicable to the design, but require use of a computer that may not always be available to office practice.

As has been mentioned above, the distribution of lateral forces between the frames and the walls should result in more economical structures because, in practical cases, the results of an exact analysis will indicate a reduction of reinforcement in the shear wall. On the other hand, the building code requirement (6) of the one-third increase in allowable wind or earthquake stresses will generally permit accommodation of the additional stresses in the frame with no need for additional reinforcement over the major part of most tall structures.

Recent building regulations are influenced by the concept that structures designed for earthquake regions must serve two functions; (1) for frequent small shocks, they must be capable of controlling damage to nonstructural elements in a building (partitions, skin, ducts, water and soil lines, etc., which, incidentally, may amount to more than 70% of the cost of the building), and (2) for several earthquakes, the structure must have adequate ductility to accommodate large lateral deflections, with little, if any, loss in capacity. The design procedure presented in this thesis with consideration of code requirements relating to lateral loading will result in the shear wall braced structures accomplishing both functions (1) and (2) outlined above. The design information presented in Khan's article (1) is helpful to engineers to establish more precise and economical reinforcing requirements. But the moment distribution is very time consuming for multibayed multistory buildings. Moreover, the design procedure requires successive adjustments to story deflections, so that it too is iterative.

An attempt has been made to both simplify and abbreviate existing techniques by combining methods suggested in recent literature, with the care not to dissatisfy the equilibrium conditions (Chapter 3).

Base rotation is considered in Chapter 4 in order to determine its effect on the moments and shears in the final solution. An investigation is made also into the rate of closure of the iteration when Khan's charts (1) are not used to get the deflected shape close to the final correct deflected shape.

Although the analytical method considered is applicable for free-standing walls, or the enclosure around elevator shaft or stairs, it is not applicable to walls that are filled-in panels bounded by steel framing. The constraints imposed by the boundary connections by the frame would prevent, or modify, deflection as a contilever. Similarly the presence of such filled-in walls would modify the deflection of the frame members.

Note: The symbols adopted for use in this thesis are defined where they first appear and are listed alphabetically in Appendix II.

CHAPTER 2

THE EQUIVALENT COLUMN METHOD

A. Physical Analysis.

The interaction of a shear wall and a frame is a special case of indeterminancy in which two basically different components are tied together to produce one structure. If the frame alone is considered to take the full lateral load, it would develop moments in columns and beams to resist the total shear at each story while the effects of overturning would normally be considered secondary and, in most cases, negligible. In resisting all lateral loads, a frame would deflect as in Fig. 1(a). The floors would remain essentially level even though the joints would rotate. If a shear wall, on the other hand, is considered to resist all the lateral loads, it would develop moments at each floor equal to the overturning moment at that level and the deflected shape, Fig. 1(b) would be that of a cantilever.

If a shear wall and a frame exist together in a building, each one will try to obstruct the other from taking its natural free deflected shape, and as a result a distribution of forces between the two results. As shown in Fig. 1(c), the frame will restrain or pull the shear wall

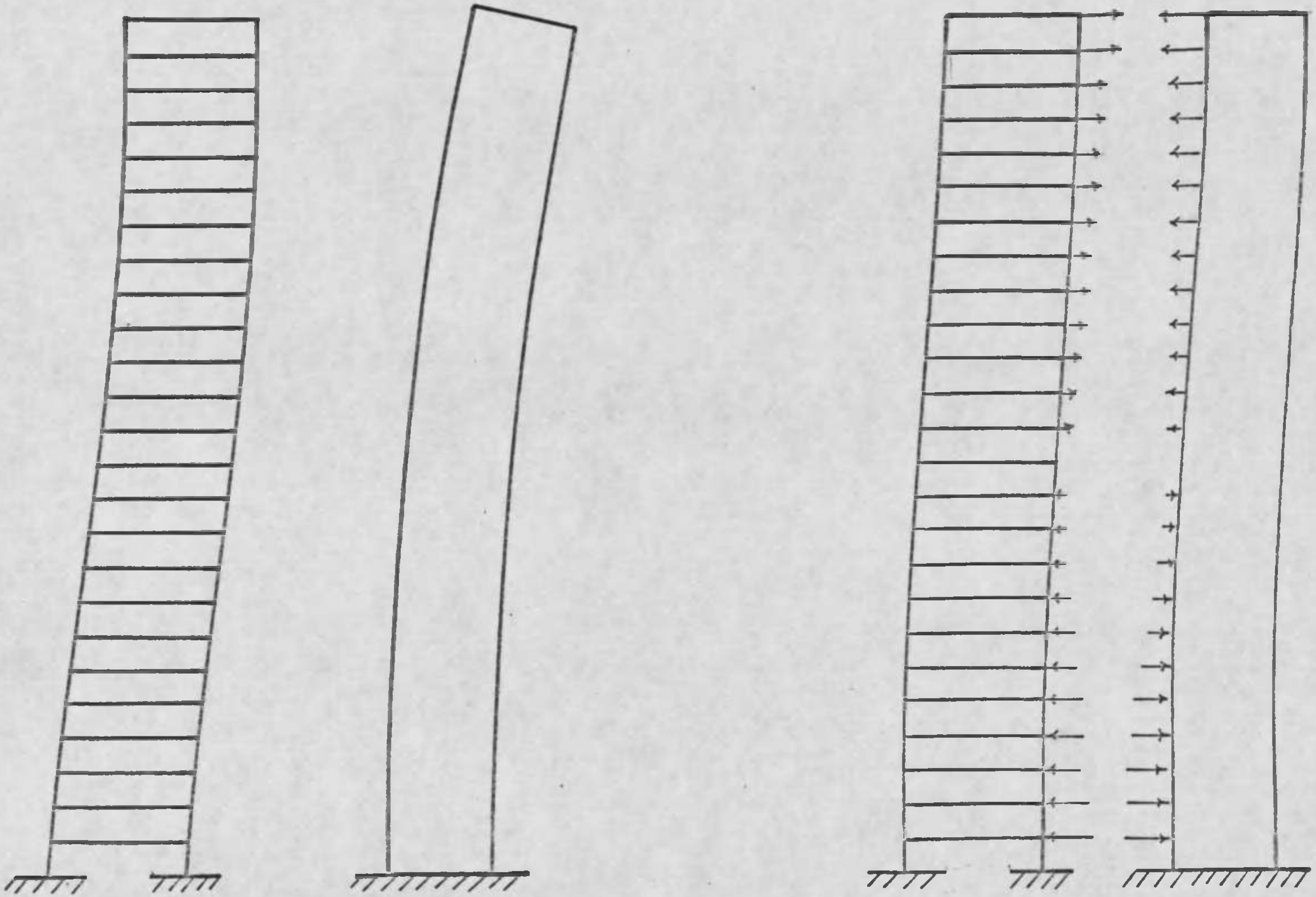

a. Free Frame   b. Free Wall   c. Combined Frame & Wall

Figure 1. Typical Deflected Shapes.

back in upper stories, while in the lower regions the opposite will occur.

The conflicting deflection characteristics of the frame and the shear wall can be considered if the structure is first divided into two separated systems (1) frame, and (2) shear wall. Then for an approximate deflected shape of the frame, the developed forces and moments are calculated at the joint between shear wall and frame at each story. The difference of forces and moments between the external loading and frame are applied to the shear wall to find the deflection of the wall at each story, and these deflections are compared with those previously assumed. The procedure is repeated until (1) horizontal deflection must be same in both systems at corresponding levels, and (2) the summation of shears developed in both systems must be equal to the total external shear (due to loading) at every story. Since this is essentially a successive approximation procedure, equality means an acceptably low level of inequality.

In this chapter, an attempt has been made to mathematically represent the frame as one cantilever and the shear wall as a second.

B. Twin Cantilevers.

Initial Assumptions

The assumptions which are usually made in the analysis of shear walls are as follows.

1. Shear walls have moment and shear resisting connections with the adjacent framework.
2. Shear walls act mainly as vertical cantilevers fixed at the footing level.
3. The entire structure is tied and braced firmly so that the building tends to act as a single unit.
4. The floor slabs are infinitely rigid in their own plane. Since the rotation is inversely proportional to the flexural rigidity, the slabs are considered not to undergo any rotation or distortion in the horizontal plane. But in case of flat slab design, the slab does undergo flexure in the vertical plane. Thus, the method is still valid for flat slab design.
5. Initially, it is assumed that the slopes in the frame at any particular floor are the same; also that the slopes in the walls at any floor level are the same though different from that in the frame.

Method of Analysis:

The building consisting of frames and walls is replaced by two representative cantilevers (Fig. 2). The substitute cantilever for the frame includes the stiffnesses of the columns and beams. The other cantilever represents the shear wall or assembly of the shear walls. These two cantilevers are tied together at each floor level so that

1. the sum of the shears at any story developed by two cantilevers is equal to the total shear acting on the building,
2. the slope at one end of the link members joining the wall and frame represents the slope in the frame work, whereas the slope at the other end represents the slope of the shear wall,
3. the lateral displacement of the two cantilevers at any floor level is the same.

Derivation of General Equations:

The basic slope deflection equations for a beam are

$$M_{AB}=k_{BA}(2d_A^f+d_B^f+U_{AB})-M^F_{AB} \quad \ldots\ldots(1)$$

$$M_{BA}=k_{BA}(2d_B^f+d_A^f+U_{BA})+M^F_{BA} \quad \ldots(2)$$

where M_{AB}= resultant end moment at point A of member AB, positive if clockwise and vice versa.

M^F_{AB}= fixed end moment at point A of member AB, positive if clockwise and vice versa.

d^f_A = $2E\theta_A$= deformation at A

Referring to Fig. 2(a), for joint n, for equilibrium to exist.

$$M_{n,n-1}+M_{n,n+1}+M_{n,n'}+M_{n,n''}=0 \quad \ldots\ldots(3)$$

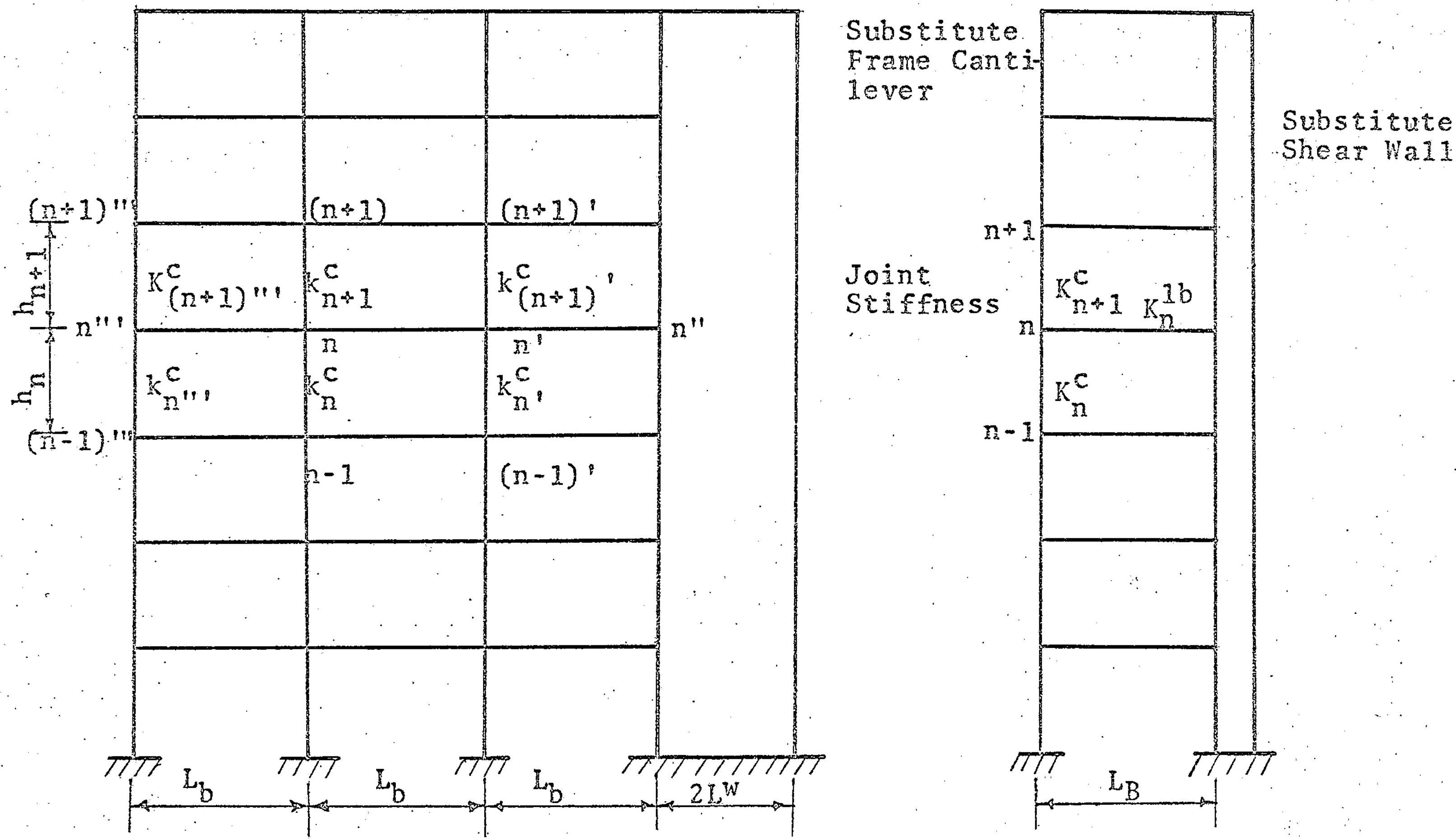

a. Shear-Walled Frame

b. Twin Cantilevers

Figure 2. Substitute Cantilevers

Expressing the above relations in terms of the slope deflection equations (1) and (2).

$$k_n^c(2d_n^f+d_{n-1}^f+U_n^f)+2k_{n+1}^c(2d_n^f+d_{n+1}^f+U_{n+1}^f)+k_{n'}^b(2d_n^f+d_{n'}^f)$$
$$+k_n^b(2d_n^f+d_{n'''}^f)=0.$$

Where, k_n^c= stiffness of columns between floor n and n-1

$U_n^f= -\frac{6ED_n}{h_n}$ $\quad$ D_n= relative displacement of the two ends of member n

E = modulus of elasticity

h_n= height of nth story

k_n^b= stiffness of beam at nth floor.

But as per assumption, 5,

$$\theta_{n'}^f=\theta_{n'''}^f=\theta_n^f \rightarrow d_{n'}^f=d_{n'''}^f=d_{n'}^f$$

Where θ_n^f= joint rotation of frame work at nth floor.

So, substituting this deformation condition in previous equation

$$d_n^f(2k_n^c+2k_{n+1}^c+3k_n^b+3_{n'}^b)+k_n^c d_{n-1}^f+k_{n+1}^c d_{n+1}^f+k_n^c U_n^f$$
$$+k_{n+1}^c U_{n+1}^f=0\ldots\quad\ldots(4)$$

Similarly for equilibrium to exist at joint n''',

$$d_n^f(2k_{n'''}^c+2k_{(n+1)'''}^c+3k_n^b)+k_{n'''}^c d_{n-1}^f+ k_{(n+1)'''}^c d_{n+1}^f$$
$$+k_{n'''}^c U_f^n+k_{(n+1)'''}^c U_{n+1}^f=0\ldots\quad\ldots(4a)$$

For equilibrium to exist at joint n',

$$M_{n',(n+1)'}+M_{n',(n-1)'}+M_{n',n''}+M_{n'',n}=0\ldots \quad \ldots(5)$$

There will be vertical movements at the connecting points of the "link" beams with the shear wall. The vertical movement at any connecting point will be equal to the slope at that point multiplied by half the width of the shear wall. Vertical movement at point $n''=-\theta^{w}_{n''}\ell^{w}_{n}$,

where $\theta^{w}_{n''}$= rotation of shear wall at nth floor

ℓ^{w}_{n} = half the width of an actual shear wall at nth floor.

So, $U_{n',n''}=\dfrac{6E\theta^{w}_{n'}\ell^{w}_{n}}{\ell^{b}_{n}}$

$$=\frac{3\ell^{w}_{n}d^{w}_{n}}{\ell^{b}_{n}}\ .$$

Now expressing equation (5) in terms of the slope deflection equations (1) and (2)

$$k^{c}_{(n+1)'}(2d^{f}_{n'}+d^{f}_{(n+1)'}+U^{f}_{n+1})+k^{c}_{n'}(2d^{f}_{n'}+d^{f}_{(n-1)'}+U^{f}_{n})$$
$$+k^{b}_{n'}(2d^{f}_{n'}+d^{f}_{n})+k^{1b}_{n}(2d^{f}_{n}+d^{w}_{n''}+3\frac{\ell^{w}_{n}d^{w}_{n''}}{\ell^{b}_{n}})=0$$

Where, k^{1b}_{n}= stiffness of link beam

$d^{w}_{n''}$= deformation at joint between link beam and wall at nth floor.

But $d^f_{n'} = d^f_n$ $\qquad d^f_{(n+1)'} = d^f_{n+1}$

$d^f_{(n-1)'} = d^f_{(n-1)}$ $\qquad d^w_{n''} = d^w_n$

Therefore,

$$d^f_n(2k^c_{(n+1)'}+2k^c_{n'}+3k^b_{n'}+2k^{1b})+k^c_{(n+1)'}d_{n+1}$$

$$+k^c_{n'}d^f_{n-1}+k^c_{(n+1)'}U^f_{(n+1)}+k^c_{n'}U^f_n+k^{1b}_n(1+\frac{3\ell^w_n}{\ell^b_n})d^w_n = 0 \ldots \qquad \ldots (6)$$

Adding equations (4), (4a), and (6),

$$d^f_n(2k^c_n+2k^c_{n'''}+2k^c_{n'}+2k^c_{n+1}+2k^c_{(n+1)'''}+2k^c_{(n+1)'}$$

$$+6k^c_n+6k^b_{n'}+2k^{1b}_n)+d^f_{n+1}(k^c_{n+1}+k^c_{(n+1)'''}$$

$$+k^c_{(n+1)'})+d^f_{n-1}(k^c_n+k^c_{n'''}+k^c_{n'})+k^{1b}_n(1+\frac{3\ell^w_n}{\ell^b_n})d^w_n$$

$$+U^f_n(k^c_n+k^c_{n'''}+k^c_{n'})+U^f_{n+1}(k^c_{n+1}+k^c_{(n+1)'''}+k^c_{(n+1)'})=0 \ldots \qquad (7)$$

Now, making the following substitutions in equation (7)

$$K^c_n = k^c_n+k^c_{n'''}+k^c_{n'} = \Sigma k^c_n$$

$$K^c_{n+1} = k^c_{n+1}+k^c_{(n+1)'''}+k^c_{(n+1)'} = \Sigma k^c_{n+1}$$

(These are the sums of all the column stiffnesses at the nth and the n+1th stories, respectively.)

$$K_n^b = k_n^b + k_{n'}^b = \Sigma k_n^b$$

(This is the sum of the stiffnesses of all the beams except the link beams at the nth floor.)

$$K_n^{1b} = \Sigma k_n^{1b}$$

$$\overline{K_n^{1b}} = \Sigma \left[k_n^{1b}\left(1 + \frac{3\ell_n^w}{\ell_n^b}\right)\right]$$

(These are the sums of stiffnesses of all the link beams.)

$$d_n^f(2K_n^c + 2K_{n+1}^c + 6K_n^b + 2K_n^{1b}) + K_{n+1}^c d_{n+1}^f$$

$$+ K_n^c d_{n-1}^f + \overline{K_n^{1b}} d_n^w + K_n^c U_n^f + K_{n+1}^c U_{n+1}^f = 0 \quad \ldots \quad \ldots (8)$$

Say, $K_n = 2K_n^c + 2K_{n+1}^c + 6K_n^b + 2K_n^{1b}$ ... ...(8a)

Substituting equation (8a) into equation (8),

$$K_n d_n^f + K_{n+1}^c d_{n+1}^f + K_n^c d_{n-1}^f + \overline{K_n^{1b}} d_n^w + K_n^c U_n^f + K_{n+1}^c U_{n+1}^f = 0 \ldots \quad \ldots (9)$$

Equation (9) shows that the structure shown in Fig. 2(a) can be represented as shown in Fig. 1(b). Thus the frame system can be represented as one cantilever and the assembly of shear walls as the other. These twin cantilevers are tied together by link beams so that the entire structure is looked at as a single unit. K_n(Eqn. 8a) is the stiffness of the joint between frame column and link beam at nth story.

CHAPTER 3

INTERACTION OF SHEAR WALLS AND FRAMES

A. Concept and Method of Analysis.

As has been seen in Chapter 2, the concept of twin cantilevers reduces the multibay, multistory shear-walled structure into the single-bay multistory shear-walled structure. Then the analysis is performed in two stages. In the first stage of analysis of the structure, it is necessary to determine the deflected shape and the amount of lateral load distributed to the walls and frame, respectively, at each story. For this purpose, the structure is separated into two distinct systems; system W and system F.

1. System W: Shear wall or assembly of shear walls. This system can have any configuration. Walls are extended over the entire height of the structure. The stiffness of this shear wall system at any story equals the sum of the stiffnesses of all shear walls regardless of their shape and size. Shape and size should be considered in computing an average ℓ_W, the distance from the neutral axis of the system W to its extreme fiber. Thus, the coupled shear walls can be represented in high multistory buildings as a single wall with an

equivalent stiffness equal to the sum of the stiffnesses of both shear walls.

2. System F: This system includes all columns and beams contributing to the lateral stiffness. The link beams, members linking the frames with the shear walls, are also included in this system. In twin cantilevers, the stiffnesses of columns, beams and link beams are simply the sum of the stiffnesses of all such members in the structure. The link beam span is an average of the link beam spans of the structure when this spans are within the same range of magnitude.

Then the analysis of a single-bay shear-walled multistory frame system is performed by an iterative solution presented subsequently.

B. Iterative Procedure to be Used.

Equilibrium conditions:

1. The horizontal deflection must be the same in both cantilevers at corresponding levels.
2. The summation of shears developed in both cantilevers must be equal to the total external shear (due to loading) at every story.
3. Link members connecting two cantilevers must undergo the same rotations and vertical translations as those of system W and system F at their point of connection.

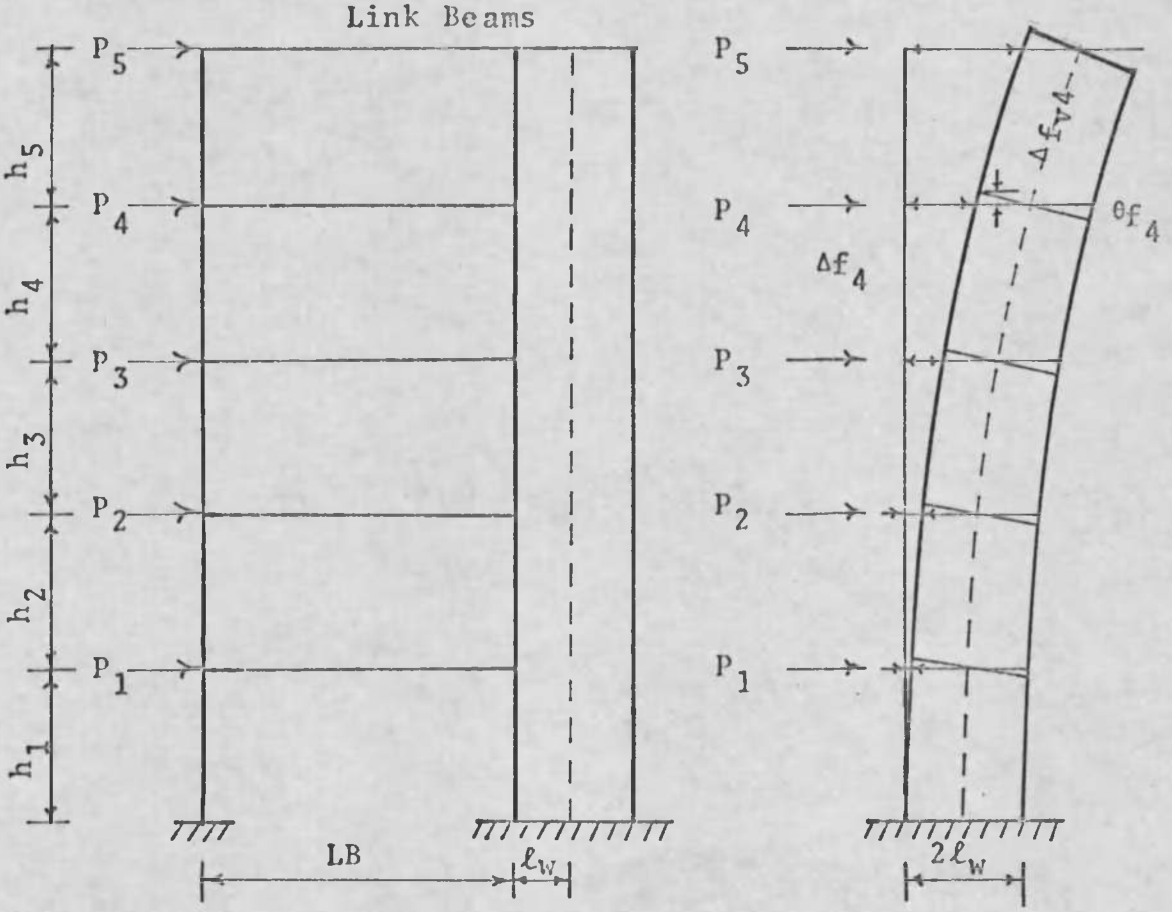

(a) Idealized Structure

(b) Free Deflection of System W.

Figure 3. Idealized Structure and Free Deflection of the Wall.

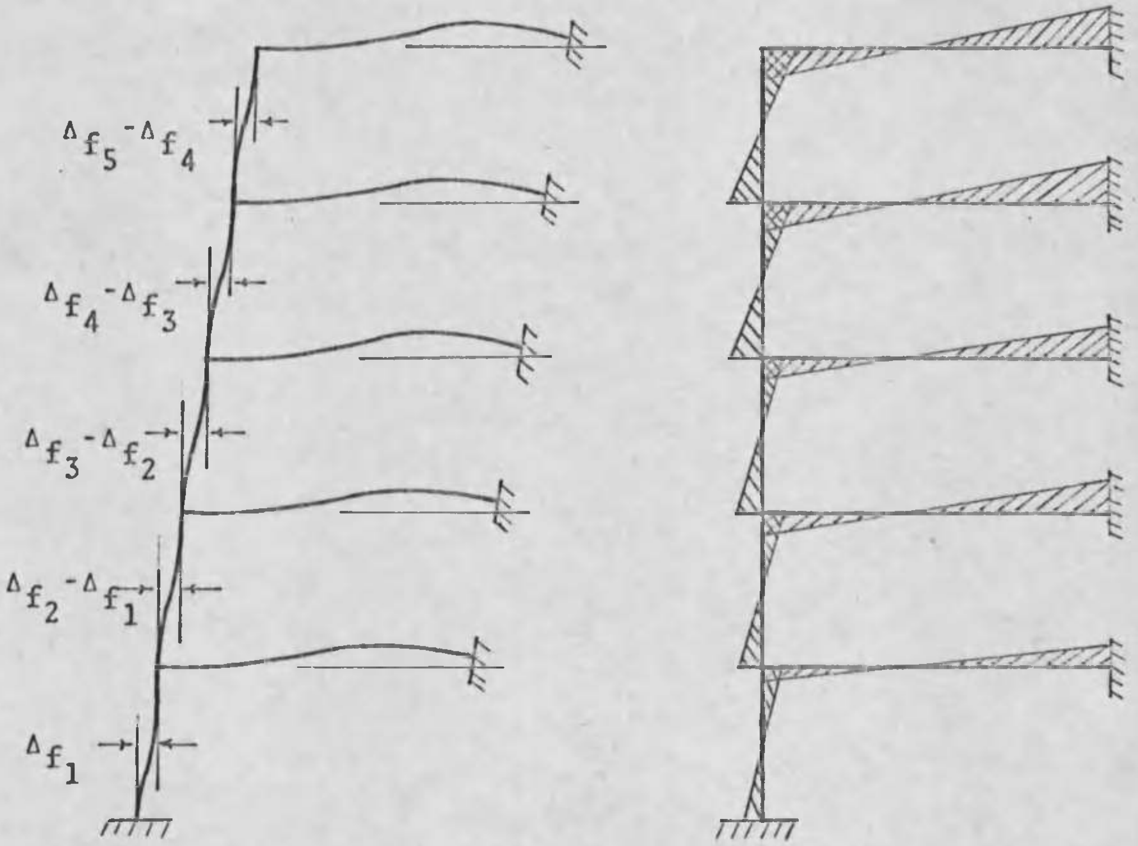

"Force-Fitting" System F

Fixed End Moment From "Force Fitting"

Figure 4. Fixed End Moments From Deflected Shape of the Frame.

The foregoing three requirements of compatibility and equilibrium can be achieved by the following six steps of analysis.

Step 1: Free Deflection of Shear Wall (conjugate beam method)

Total computed external loads (wind or seismic) on the idealized structure (Fig. 3a) are directly applied to shear wall at each floor level. The slopes and deflections of the shear wall at each floor level are determined by the conjugate beam method shown hereinafter.

Conjugate Beam Method.

In the conjugate beam method (8), the relationship between the real beam and the conjugate beam are as follows:

(a). The span of the conjugate beam is equal to the span of the real beam.

(b) The load of the conjugate beam is the M/EI diagram of the real beam.

(c) The shear at any section of the conjugate beam is equal to the slope of the corresponding section of the real beam.

(d) The moment at any section of the conjugate beam is equal to the deflection at the corresponding section of the real beam.

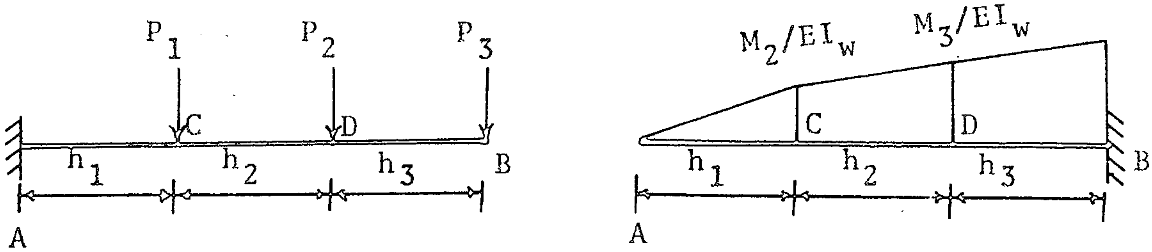

(a) Real Beam (b) Conjugate Beam

where I_w=moment of intertia of shear wall.
E =Modulus of elasticity of concrete (shear wall)

Figure 5. Shear Wall Flexural Equivalency.

The real beam is fixed at A (Fig. 5a)

$\therefore$ At end A; Rotation $\theta=0$

Deflection =0

$\therefore$ In conjugate beam; at end A shear =0

and moment=0

So end A is free in the conjugate beam as shown in Fig. 5. Similarly, in the real beam, the slope and deflection are not zero at free end B, hence the end B is fixed in the conjugate beam as shown in Fig. 5b.

For example: The slope at pt. C in the real beam;

θ_C=shear at pt. C in the conjugate beam

$$= \frac{1}{2}\,\frac{M_2}{EI_w} x h_1 = \frac{M_2 h_1}{2EI_w}$$

and the deflection at pt. C in the real beam;

Δ_C=moment at pt. C in the conjugate beam

$$=\frac{1}{2}\,\frac{M_2}{EI_w}\times h_1\times\frac{h_1}{3}$$

$$=\frac{M_2 h_1^2}{6EI_w}$$

Thus, the free horizontal deflection and rotation can be calculated by the conjugate beam method at any point on the shear wall. The free horizontal deflection, rotation and vertical deflection at any point, i, are denoted as Δ_{fi}, θ_{fi} and Δ_{fvi} respectively. The deflections one floor above and below are $\Delta_{f(i+1)}$ and $\Delta_{f(i-1)}$ respectively.

Step 2: Initial Deflection and Rotation.

For quick convergence, initial deflection and rotations are assumed or approximated from Figs. 32 through 38 given in Khan's article (1). In the absence of a good estimate, however, the deflected shape is assumed as the free deflected shape of the shear wall, which would mean that, in the first cycle, initial deflection and rotation at the ith floor would be

$$\Delta_{ii(1)}=\Delta_{fi}$$

and

$$\theta_{ii(1)}=\theta_{fi}.$$

System F is forced to undergo the assumed deflections at each floor (Fig. 4a). This also requires that the connecting members at each floor must have the same rotations and vertical translation as system W at their points of connection with system W.

Step 3: Induced Fixed End Moments.

The moments induced by "force-fitting" can be determined directly by using moment distribution. The forced-fitted frame shown in Fig. 4a has known story deflection and rotations at the connecting points; hence, for uniform columns and beam sections, the fixed end moment at the beginning of moment distribution (Fig. 4b) would be for columns at ith story

$$FM_{ci}=\left(\frac{6EI_{ci}}{h_i^2}\right)(\Delta_i-\Delta_{i-1}).$$

At the ith floor for "link" beams at their shear wall end,

$$FM_{biw}=\left(\frac{4EI_{bi}}{L_b}\right)\theta_i+\left(\frac{6EI_{bi}}{L_b^2}\right)\Delta_{vi}$$

but $\Delta_{vi}=\ell_w\theta_i$

$$\therefore\ FM_{biw}=\left(\frac{2EI_{bi}}{L_b}\right)\left[2+3\left(\frac{\ell_w}{L_b}\right)\right]\theta_i$$

and at the ith floor for "link" beams at their frame end

$$FM_{bif}=\left(\frac{2EI_{bi}}{L_b}\right)\theta_i+\left(\frac{6EI_{bi}}{L_b^2}\right)\Delta_{vi}.$$

But again $\Delta_{vi}=\ell_w\theta_i$

$$\therefore FM_{bif} = \left(\frac{2EI_{bi}}{L_b}\right)\left[1+3\left(\frac{L_s}{L_b}\right)\right]\theta_i .$$

Distribution Factors:

As has been seen in Chapter 2, the joint stiffness, in the twin cantilever, at any nth joint is as follows:

$$K_n = 2K_n^c + 2K_{n+1}^c + 6K_n^b + 2K_n^{1b} .$$

Therefore,

Distribution Factors:

$$\text{Lower column} = \frac{2K_n^c}{K_n} = \frac{2K_n^c}{2K_n^c + 2K_{n+1}^c + 6K_n^b + 2K_n^{1b}}$$

$$\text{Upper column} = \frac{2K_{n+1}^c}{K_n} = \frac{2K_{n+1}^c}{2K_n^c + 2K_{n+1}^c + 6K_n^b + 2K_n^{1b}}$$

$$\text{Link beam} = \frac{2K_n^{1b}}{K_n} = \frac{2K_n^{1b}}{2K_n^c + 2K_{n+1}^c + 6K_n^b + 2K_n^{1b}} .$$

Knowing the fixed end moments and the distribution factors, the moment distribution can be run to get final moments in the members. When a known, fixed sidesway is imposed on a structure, as in this case, the cumbersome sidesway corrections to the moment distribution are not required, and the solution will converge rapidly.

Step 4: Story Shears in Frame.

After force-fitting system F to system W, the total shears in each story of system F as well as moments and reactions applied on system W by the connecting links are computed (Fig. 6a). The shears generated by force-fitting can be used directly in the next step. The resulting horizontal forces P' are shown in Fig. 6 only for illustration purposes. These interaction forces may be either positive or negative at different floors.

Step 5: Concentrated Moments and Net Deflections.

All shear forces and moments generated by force-fitting system F are applied to the isolated free system W (Fig. 6b). At any story i, M_i and R_{vi} should be replaced by moment (Fig. 6c)

$$M' = M_i + R_{vi} \ell_w.$$

The moments and forces shown in Fig. 6b will cause negative deflections and rotations of system W, Δ_{ai} and θ_{ai} respectively. The balance of forces and moments (loading and frame) are applied to the shear wall in order to find the net deflections and rotations, Δ_{ei} and θ_{ei} respectively at each story. So at the end of first cycle, the deflections and rotations equations can be written as follows:

$$\Delta_{ei(1)} = \Delta_{fi} - \Delta_{ai(1)}$$

$$\theta_{ei(1)} = \theta_{fi} - \theta_{ai(1)}$$

or in general at the end of the nth cycle

$$\Delta_{ei(n)} = \Delta_{ii(n)} - \Delta_{ai(n)}$$

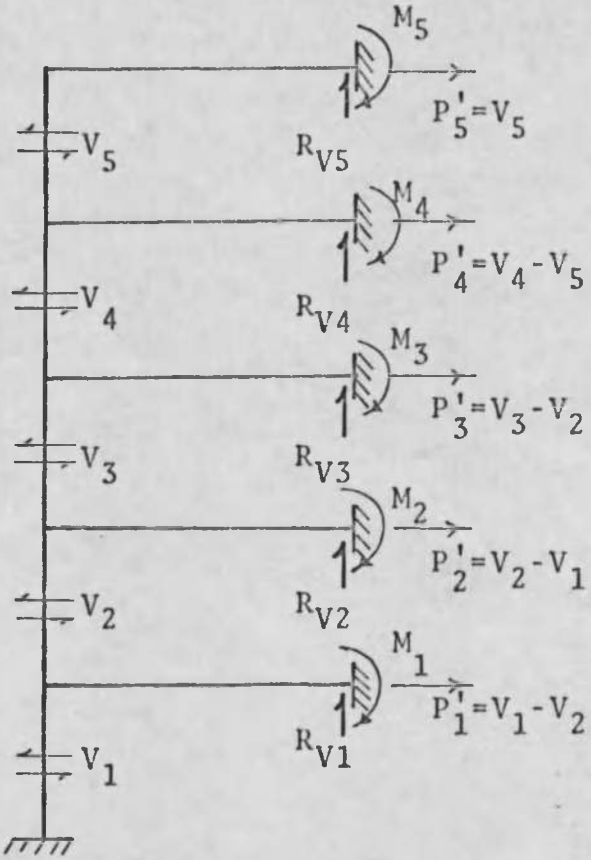

(a) Forces and Moments in System F after Moment Distribution.

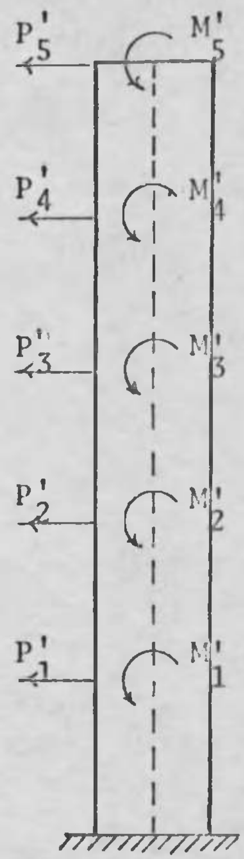

(b) Forces and Moments From System F Applied to System W.

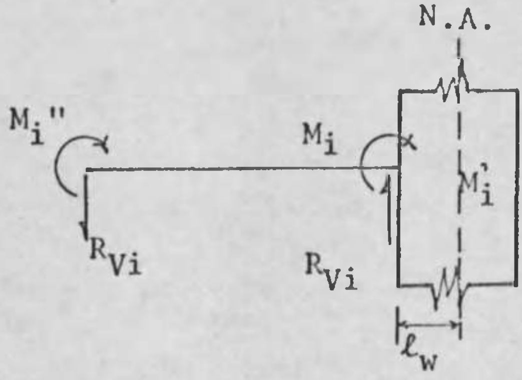

$$M_i' = M_i + R_{Vi}(\ell_w)$$

(c) Total Concentrated Bending Moments.

Figure 6. Interacting Forces and Moments of Combined System.

and

$$\theta_{ei(n)} = \theta_{ii(n)} - \theta_{ai(n)}.$$

This is the end of one cycle of iteration. For the stable condition to occur, the initial deflections at any floor "i" at the beginning of nth cycle, $\Delta_{ii}(n)$ must be the same as the end (net) deflections $\Delta_{ei(n)}$ at the completion of the nth cycle. However in many cases in the first cycle, Δ_{ei} is negative indicating that the iteration is divergent. The generalization of this method of solution therefore depends on the use of a proper "forced - convergence - correction" to be applied to the initial deformations of the nth cycle $\Delta_{ii(n)}$ and $\theta_{ii(n)}$, to obtain the initial trial deformations of the (n+1)th cycle, $\Delta_{ii(n+1)}$ and $\theta_{ii(n+1)}$.

In Fig. 6b it will be noted that the axial effects of the link beam reactions (R_{vi}) on the shear wall are neglected. This is compatible with the neglect of axial forces in most frame analysis methods. The two major contributors to shear wall behavior (concentrated moment M_i, and horizontal loading, P_i) are considered.

Step 6: The Forced Convergence Corrections.

The convergence corrections are derived from the hypothesis that in each cycle the movement of system W at each floor with respect to its free deflected shape is lineally proportional to the movement of system F with respect to the vertical line. Therefore, it can be shown that if at the nth cycle the initial trial values at the ith floor were $\Delta_{ii(n)}$ and $\theta_{ii(n)}$ and the end values were $\Delta_{ei(n)}$ and $\theta_{ei(n)}$, the initial trial values at the (n+1)th cycle should be as follows:

$$\Delta_{ii(n+1)}=\Delta_{ii(n)}+\frac{\Delta_{ei(n)}-\Delta_{ii(n)}}{1+\frac{\Delta_{fi}-\Delta_{ei(n)}}{\Delta_{ii(n)}}}$$

and

$$\theta_{ii(n+1)}=\theta_{ii(n)}+\frac{\theta_{ei(n)}-\theta_{ii(n)}}{1+\frac{\theta_{fi}-\theta_{ei(n)}}{\theta_{ii(n)}}}$$

The values Δ and θ obtained by above two equations are used as initial values for the next cycle, and the procedure is repeated beginning with the second step outlined previously. This iterative procedure is carried on until the net deflection $\Delta_{ei(n)}$ is equal to the initial deflection $\Delta_{ii(n)}$. At the end of each cycle, Δ_{ei} and Δ_{ii} should be checked until the convergence is within a specific acceptable tolerance, for example 5% to 10%, based on the designer's judgment.

Design Example:

Data: The dimensions and lateral forces are shown in the Fig. 7; whereas the elastic properties are listed as follows:

Column Stiffness $k^c=800$ in^3

Beam Stiffness $k^b=200$ in^3

Shear Wall $k^{1b} = 200\ in^3$

$I = 200\ ft^4$

Area $A = 30\ ft^2$

$E = 3420 K/in^2$

As has been seen in Chapter 2, the structure shown in Fig. 7 can be represented as the single bay shear-walled frame structure (Fig. 8).

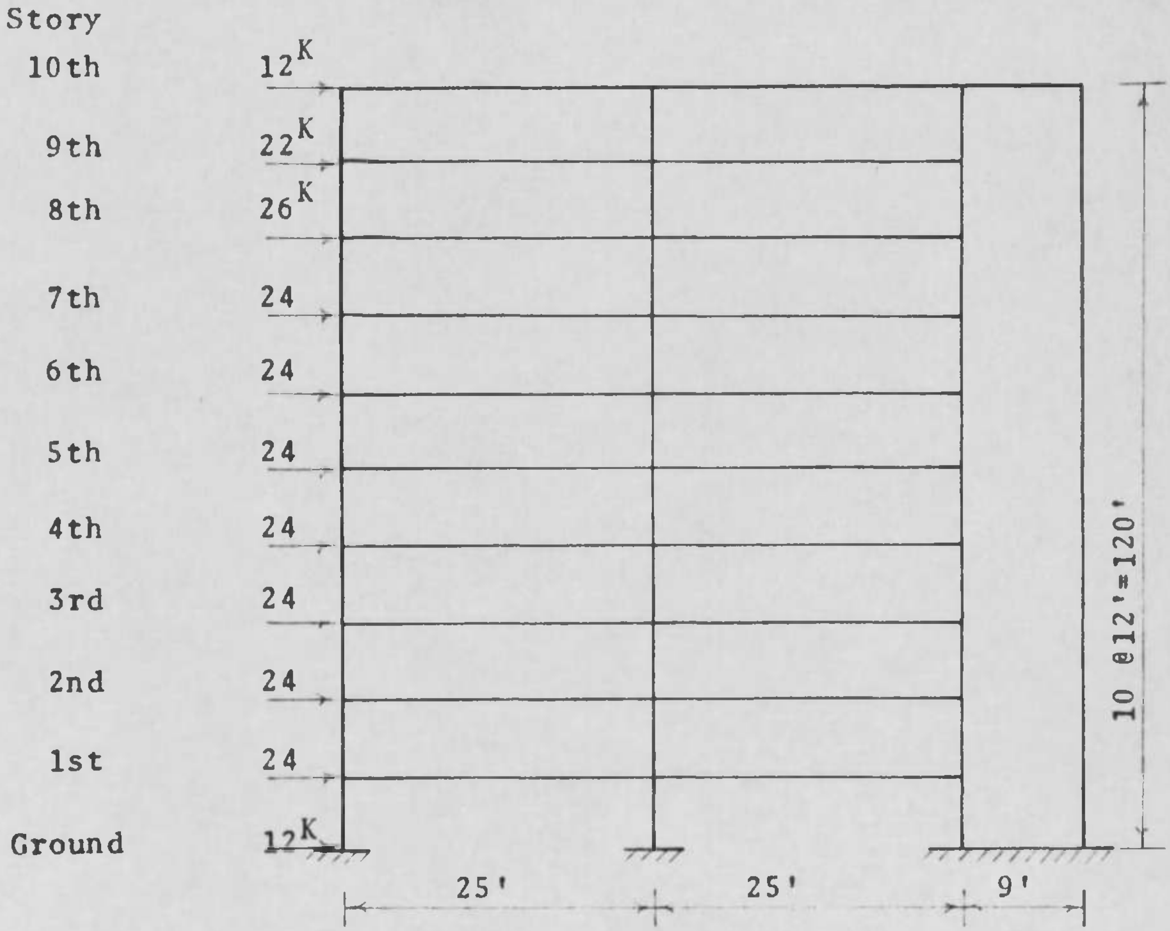

Figure 7. Shear Walled Frame Elevation for Illustrated Example.

Where $K^c = \Sigma k^c = 800+800$

$= 1600 \text{ in}^3$

$K^{1b} = \Sigma k^{1b} = 200 \text{ in}^3$

$= 200 \text{ in}^3$

Joint stiffness at any joint "n"

$$K_n = 2K_n^c + 2K_{n+1}^c + 6K_n^b + 2K_n^b$$

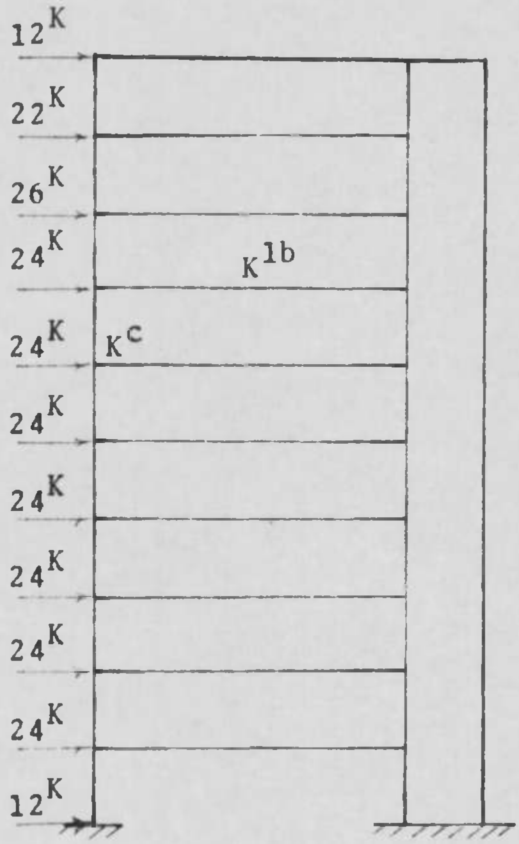

Figure 8. Substitute Cantilevers for Illustrated Example.

$\therefore$ For top joint $K_{10} = 2(1600) + 2(0) + 6(200) + 2(200)$

$= 3200 + 0 + 1200 + 400$

$= 4800 \text{ in}^3$

For any intermediate joint

$$K_n = 2(1600)+2(1600)+6(200)+2(200)$$
$$=3200+3200+1200+400$$
$$=8000 \text{ in}^3$$

Distribution Factors

Top joint: $\text{link beam} = \dfrac{2K^{1b}}{K_{10}} = \dfrac{2\times 200}{4800} = 0.08$

$$\text{Column} = \frac{2K_n^c}{K_{10}} = \frac{2\times 1600}{4800}$$

$$=0.33$$

Intermediate joint: $\text{link beam} = \dfrac{2K_n^{1b}}{K_n}$

$$=\frac{2\times 200}{8000}$$

$$=0.05$$

Upper or lower col. $=\dfrac{2K_n^c}{K_n}$

$$=\frac{2(1600)}{8000}$$

$$=0.4$$

Free Deformations of Shear Wall.

Neglecting the frame, at the first stage, the external lateral loads are applied to the shear wall and thus free deflections and rotations are calculated in

Appendix I(A) at each floor level. These deflections and rotations are tabulated in Table 1. The third column of Table 1 shows the factors from Khan's (1) chart in order to approximate the deflected shape close to the final deflected shape of the structure. The deflected shape of the force-fitting system is shown in Fig. 4a.

Table 1. Horizontal Deflection and Rotation for First Iterative Trial.

Story	Free Deflection Δ_{if}	Free Rotations θ_{if}	Reduction Factor F	$\Delta_{ii(1)}$	$\theta_{ii(1)}$
1	0.13	.00158	.006	0.04	.000034
2	0.46	.00285	.022	0.14	.000125
3	0.96	.00364	.045	0.287	.000255
4	1.57	.00440	.077	0.49	.000436
5	2.28	.00493	.110	0.70	.00063
6	3.05	.00527	.150	0.955	.00087
7	3.86	.0055	.193	1.23	.00109
8	4.69	.0056	.234	1.49	.00132
9	5.53	.00565	.280	1.782	.00158
10	6.37	.00566	.325	2.07	.00184

The force-fitting system is shown in Fig. 4a.

The induced moment in link beam at shear wall end

$$FM_{biw}=(2EK_{bi})(2+3\frac{L_s}{L_b})\theta_i$$

$$=\frac{2\times 3420\times 200}{12}(1+3\frac{4.5}{25})\theta_i$$

$$=114\times 10^3(2.54)\theta_i$$

$$=289.56\times 10^3\theta_i$$

At 10th story

$\therefore FM_{b10w}=289.56\times10^3\times.00184$

$=533$ K Ft.

Similarly

$FM_{bqw}=457$ K Ft.

$FM_{b8w}=384$

$FM_{b7w}=315$

$FM_{b6w}=252$

$FM_{b5w}=182$

$FM_{b4w}=126$

$FM_{b3w}=73.8$

$FM_{b2w}=36.2$

$FM_{b1w}=9.83$

Now induced fixed end moment in link beam on frame end.

$$FM_{bif}=2EK_{bi}(1+3\frac{L_s}{L_b})\theta_i$$

$$=\frac{2\times3420\times200}{12}(1+3\frac{4.5}{25})\theta_i$$

$$=114\times1.54\times10^3\theta_i$$

At the 10th story

$$FM_{b10f}=114\times1.54\times10^3\times.00184$$
$$=323\text{ KFt.}$$

Similarly

$FM_{b9f}=277$ K.Ft.

$FM_{b8f}=232$

$FM_{b7f}=191$

$FM_{b6f}=153$

$FM_{b5f}=110$ KFt.

$FM_{b4f}=76.3$

$FM_{b3f}=44.7$

$FM_{b2f}=22.0$

$FM_{b1f}=5.95$

<u>Induced F.E.M in Columns</u>

At any story i,

$$FM_{ci}=\frac{6EI_c}{h_i^2}(\Delta_i-\Delta_{i-1})$$

$$=\frac{6EK_c}{h_i}(\Delta_i-\Delta_{i-1})$$

$$=\frac{6\times3420\times1600}{12\times12\times12}(\Delta_i-\Delta_{i-1})$$

$$=19\times10^3(\Delta_i-\Delta_{i-1})$$

At 10th Story

$FM_{c10}=19\times10^3(2.07-1.782)$

$=5470$ K.Ft.

Similarly:

$FM_{c9}=5540$ K'

$FM_{c8}=4940$ K'

$FM_{c7}=5220$ K'

$FM_{c6}=4840$ K'

$FM_{c5}=3990$ K'

$FM_{c4}=3860$ K'

$FM_{c3}=2790$ K'

$FM_{c2}=1900$ K'

$FM_{c1}=760$ K'

After running the moment distribution (see Appendix I(B), the final forces and moments are shown in Fig. 9. The story shears in the frame and the shear wall, concentrated bending moment and then final bending moments are tabulated in the Table 2.

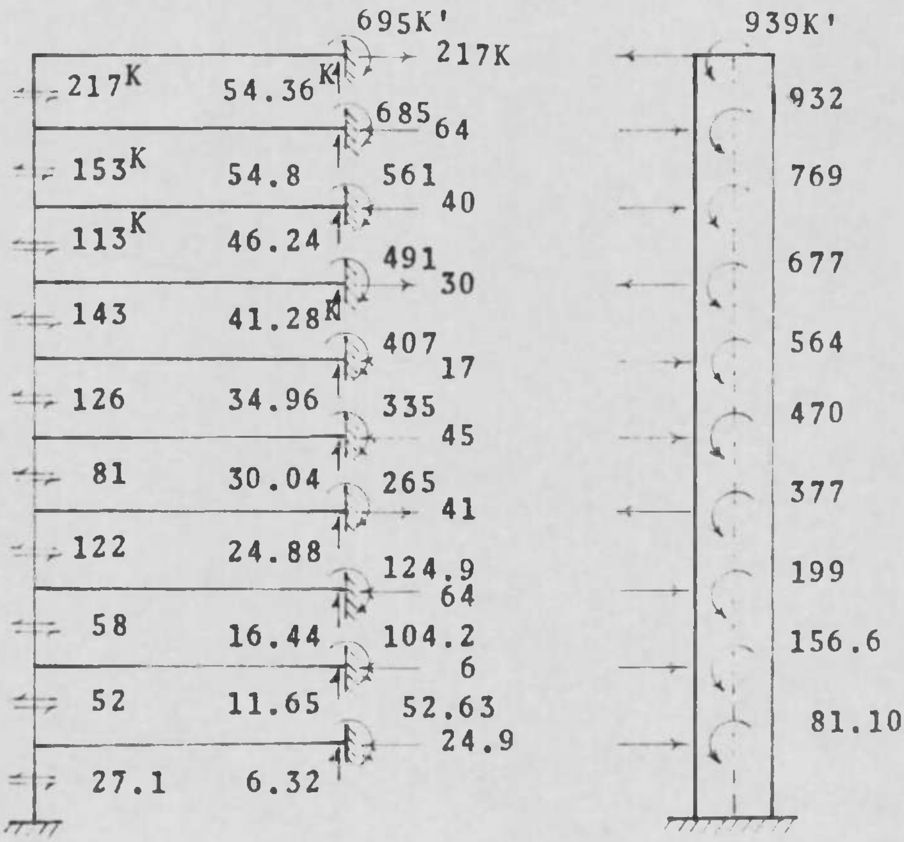

Figure 9. Forces and Moments After Moment Distribution.

Table 2. Final Bending Moment on the Wall at the End of 1st Trial.

Story	External Shears Kips	Frame Story Shears Kips	Story Shear in Wall Kips	Conc. Bending Moments K'	Final Bending Moments K'
10th	12	217	-205	939	939
9th	34	153	-119	932	4331
8th	60	113	- 53	769	6528
7th	84	143	- 59	677	7841
6th	108	126	- 18	564	9113
5th	132	81	51	470	9893
4th	156	122	34	377	9658
3rd	180	58	122	199	9449
2nd	204	52	152	156.6	8141
1st	228	27.1	200.9	81.10	6398.7
Ground	240	0	212.9	0	3988

The final moments will give the net deformations of the shear wall at the end of the first trial, $\Delta_{ei(1)}$ and $\theta_{ei(1)}$. The calculations for these net deformations are done by conjugate beam method and tabulated in Table 6 in Appendix I(C).

<u>Deformations for Second Cycle.</u>

The initial trial values for the next cycle is obtained as follows:

$$\Delta_{ii(n+1)}=\Delta_{ii(n)}+\frac{\Delta_{ei(n)}-\Delta_{ii(n)}}{1+\frac{\Delta_{fi}-\Delta_{ei(n)}}{\Delta_{ii(n)}}}$$

$$\therefore \left\{ \Delta_{ii(2)}=\Delta_{ii(1)}+\frac{\Delta_{ei(1)}-\Delta_{ii(1)}}{1+\frac{\Delta_{fi}-\Delta_{ei(1)}}{\Delta_{ii(1)}}} \right.$$

For example at 10th story

$$\Delta_{i10(2)}=2.07+\frac{-7.14-2.07}{1+\frac{6.37-(-7.14)}{2.07}}$$

$$=2.07-1.22$$

$$=0.85 \text{ in.}$$

Similarly for all the stories the deflections and rotations are calculated, and the results are shown in Table 6 (Appendix I(C).

This iterative procedure is carried on until the initial deflections $\Delta_{ii(n)}$ are equal to the final deflections $\Delta_{ei(n)}$. [The results of intermediate iterations are tabulated in Appendix C, Table 7 through Table 11.]

The final results are tabulated and compared with those obtained by Khan's Method in Table 3.

Table 3. Final Results

Floor	Shear Wall only; Cantilever Analysis			Proposed Method				Khan's Method			
	Shear Kips	Bending Moments K'	Deflection in.	Shear Kips	Bending Moment K'	Concentrated Bend Mom. K'	Deflections in.	Shear Kips	Bend Mom K'	Concentrated B.M. K'	Deflections in.
10	12	0	6.37	-27.1	173	173	0.89	-27.1	169.8	169.8	0.92
9	34	-144	5.53	- 9.0	704.2	206.5	0.83	- 7	699.0	204.0	0.86
8	60	-552	4.69	39.2	1055.2	242.5	0.76	40.2	1012.0	229.0	0.79
7	84	-1272	3.86	13.0	877.3	292.5	0.69	13	815.6	286.0	0.71
6	108	-2280	3.05	68.6	1063.8	342.5	0.59	69.7	996.3	336.7	0.61
5	132	-3576	2.28	56.5	624.6	384	0.49	57.7	535.3	375.3	0.50
4	156	-5160	1.57	97.5	359.1	412.5	0.37	98	248.8	406.0	0.38
3	180	-7032	0.96	104.0	-406.4	404.5	0.25	105	-529.2	398.0	0.25
2	204	-9192	0.46	153.5	-1291.9	362.5	0.13	154	-1432.7	356.5	0.13
1	228	-11640	0.13	192.6	-2898	235.2	0.04	192.6	-3056.2	224.5	0.04
Ground	240	-14376	0	204.6	-5209.2	0	0	204.6	-5368.2	0	0

CHAPTER 4

BASE ROTATION

A. Base Rotation (General).

The engineer is sometimes confronted with the question of whether the shear wall bases should be fixed or free to rotate. At the other times he is compelled to design the footings for a central load and a moment, and for a limited amount of rotation. Therefore an understanding of the rotation characteristic of the shear wall base and footing is essential.

When the lower end of a shear wall is subjected to a bending moment, the joint between the shear wall and the footing must be strong enough to transfer the stresses. But this can be overcome by embedding dowels in the footing, and then the shear wall can be considered fully fixed to the footing. Once the shear wall is fixed to the footing, the base rotation of the shear wall is caused only by the elastic deformation due to the greater soil compression at the toe of the base, which is generally small and insignificant.

Regardless of degree of fixity between the shear wall base and the footing, the moment from the shear wall will cause unsymmetrical soil pressure. The soil pressure is assumed to have straight line or planar distribution. Unfortunately the pressure distribution is not likely to be planar and cannot be determined quantitatively (10). Therefore, the rotation of a footing acted on by a moment or an eccentric loading can only be estimated on the basis of some simple calculations guided by good engineering judgment. For example, small and shallow footings on sand are prone to rotation because the sand readily runs out from under the toe of the footing. If the footing is located at greater depth, the sand is subjected to a confining pressure due to the weight of the overlying soil. The relative effect of the edge condition diminishes as the size of footing increases. It becomes apparent that small and shallow footings on granular soils should not be relied upon for providing fixity to the shear wall base.

Contrary to the sand, clay and clayey soils resemble elastic material and are capable of resisting a concentrated stress at the edge. Furthermore since a large portion of the settlement of footings on clay is due to consolidation resulting from bending moment acting for a long period of time, so the bending moment due to the wind or seismic load acting in short duration would not cause significant rotation.

Overturning Moment.

The axial load from earthquake force on vertical elements and footings in every building or structure may be modified and the overturning moment M_b at the base of the building or structure shall be determined in accordance with the following formula.

$M_b = J\Sigma F_i h_i$ ... ...Uniform Building Code Sec. 2314, p. 115

$= J \times$ Cantilever Moment

where, $J = \frac{0.5}{\sqrt[3]{T^2}}$

and $T = \frac{.05H}{\sqrt{D}}$

F_i = Lateral force applied to a level designated as "i"

h_i = Height in feet above the base to the level designated as "i".

D = Dimension of the building in feet in a direction parallel to the applied forces.

H = The height of the main portion of the building in feet above the base.

The required value of "J" shall not be less than 0.33 nor more than 1.00. "J" should be 1.00 for elevated tank supported with four or more cross braced legs.

Base Rotation Formula.

The joint between shear wall and footing is assumed to be strong enough so that the stresses due to bending moment at the lower end of the shear wall would be transferred to the soil.

$$\text{Max stress in soil} = \frac{M_b c}{I_f}$$

where c = half length of the footing

I_f = mom. of inertia of footing.

Now,

$$\text{max. vertical defermation in soil} = \frac{M_b c}{I_f k}$$

where k = subgrade soil modulus in lbs. per sq. in. per inch of deformation.

$$\text{Base rotation: } \theta_B = \frac{\text{settlement}}{c}$$

$$= \frac{\frac{M_b c}{I_f k}}{c}$$

$$= \frac{M_b}{I_f k}.$$

The translation of the shear wall at the ground floor level is prevented in every step of the computations. Thus, only the appropriate rotation at the base of the shear wall will be permitted. The design loads can be applied directly to the shear wall, and the iterative analysis should give the desired results.

Design Example.

So far it has been assumed that full fixity exists at the base of the shear wall as in the numerical example presented in the previous chapter. However, the theory can be expanded to include the case where the base can rotate due to elastic support. This may occur if the supporting soil is elastic or if the wall is resting on columns which may have uneven settlements. In either case, a horizontal movement at the base is considered prevented.

The base rotation can easily be included in the aforementioned iterative solution by increasing the rotation at all stories by the amount of base rotation and increasing horizontal deflection at all stories by the product of base rotation and the distance from the base to each story.

In the previous example,

Cantilever mom.=-14376 K.Ft.

overturning mom. $=J\Sigma F_z h_z$

$=J\times$cantilever moment.

But $J=\dfrac{0.5}{\sqrt[3]{T^2}}$

and $T=\dfrac{.05H}{\sqrt{D}}$

$=\dfrac{.05(120)}{\sqrt{(59)}}=\dfrac{6}{7.67}$

$=0.78$

$\therefore\ J=\dfrac{0.5}{\sqrt[3]{(0.78)^2}}=\dfrac{0.5}{0.85}$

$=0.59$

$\therefore$ overturning moment= 0.59(-14376)

$\therefore M_b=-8480$ K.Ft.

Now, base rotation $\theta_B = \frac{M_b}{I_f K.}$

Take k average =200 $lbs/in^2/in$ (k varies between 50 and 500)

use footing size 6'×25'

$\therefore I_f = \frac{1}{12} \times 6 \times 25^3 = 7812.5\ Ft^4$

$$\theta_B = \frac{8480 \times 10^3}{7812.5(200 \times 1728)}$$

$= .0031$ radian

Horizontal deflection at any floor due to base rotation	=Base Rotation× Distance in inches from base to that floor.
∴Hor. Defl$^{\underline{n}}$. at 10th floor due to base rotation	$=0.0031 \times (120 \times 12)$ =4.5 in.

In the same way, the horizontal deflections due to base rotation are found out for all stories and are tabulated in Table 4.

Once the total deflections and rotations are known, the rest of the iterative procedure is followed exactly the same way as presented in Chapter 3. The final results are tabulated in Table 5 along with the previous results obtained without inclusion of base rotation for the comparison purpose.

The overall results are very close in both cases, with and without inclusion of base rotation.

B. Omission of Khan's Charts.

In this chapter, the numerical example includes the effect of base rotation of the shear wall, as well as the effect on rate of convergence if Khan's charts (1) are not used to obtain approximate deflections for each trial.

Starting with total free deflected shape, seven iterative trials have been made. The initial and net deflection versus numbers of trials graphs are plotted for each story, and these seemingly converging graphs are extrapolated to a point of intersection. These intersecting values of deflections are very close to the correct values. In the same way, the approximate values of rotations are also obtained. For the ninth, fifth and second stories these deflection and rotation graphs (Fig. 10 to Fig. 15) are presented for illustration purposes. Beginning with these close values of deflections and rotations, two more trials were needed and the subsequent third trial is the final solution. The example in the previous chapter with the exclusion of the base rotation also needed seven trials to come to the final solution even when using Khan's charts values.

This demonstrates that the technique of using the deflected shape obtained from the developed graphs from the results of the example itself converges as fast as the use of Khan's charts.

Some Δ_i and Δ_e curves cross rather than truly converging, as shown in Fig. 10 to 15; but this is to be expected since the deflection at each story is affected by the deflections of all other stories. The initial deflection values, as found from the relationship;

$$\Delta_{ii(n+1)} = \Delta_{ii(n)} + \frac{\Delta_{ei(n)} - \Delta_{ii(n)}}{1 + \frac{\Delta_{fi} - \Delta_{ei(n)}}{\Delta_{ii(n)}}}$$

do not reflect any effects from the other stories of the structure. By using the curve intersection points, known or extrapolated, as final deflection values, results very close to the correct values are obtained with a minimum of successive approximations.

Table 4. Total Free Horizontal Deflections and Rotations at Each Story.

(1)	Hori. Deflections Δ			Rotations θ		
	Free Δ_{fi} (2)	Due to base rotation (3)	Total Free (4)=(2)+(3)	Free θ_{fi} (5)	Base Rotation θ_B (6)	Total Free (7)=(5)+(6)
10	6.37	4.50	10.87	.00566	.0031	.00876
9	5.53	4.05	9.58	.00565	.0031	.00875
8	4.69	3.60	8.29	.00560	.0031	.0087
7	3.86	3.15	7.01	.00550	.0031	.0086
6	3.05	2.70	5.75	.00527	.0031	.00837
5	2.28	2.25	4.53	.00493	.0031	.00803
4	1.57	1.80	3.37	.00440	.0031	.0075
3	0.96	1.35	2.31	.00364	.0031	.00674
2	0.46	0.90	1.36	.00284	.0031	.00594
1	0.13	0.45	0.58	.00158	.0031	.00468
Ground	0	0	0	0	.0031	.0031

Table 5. Final Results With and Without Base Rotation.

Story	With Base Rotation: Shear K.	Concen. B.M K.Ft.	Bend'g Mom. K'	Defl^{n}. inch.	Without Base Rotation: Shear K.	Concen. B.M. K'	Bend'g Mom. K'	Deflections inch.
10	-39.7	193.2	193.2	0.88	-27.1	173	173	0.89
9	- 0.3	231.2	900.8	0.81	- 9.0	206.5	704.2	0.83
8	18.5	253.5	1157.9	0.74	39.2	242.5	1055.2	0.76
7	57.2	283.5	1219.4	0.67	13.0	292.5	877.3	0.69
6	47.4	324.0	857.0	0.60	68.6	342.5	1063.8	0.59
5	61.3	382.2	670.4	0.50	56.5	384.0	624.6	0.49
4	95.9	409.0	343.8	0.38	97.5	412.5	359.1	0.37
3	110.7	380.5	-426.5	0.26	104.0	404.5	-406.4	0.25
2	143.3	399.0	-1357.9	0.13	153.5	362.5	-1291.9	0.13
1	199.4	279.0	-2798.5	0.04	192.6	235.2	-2898.0	0.04
Ground	211.4	0	-5191.3	0	204.6	0	-5209.2	0

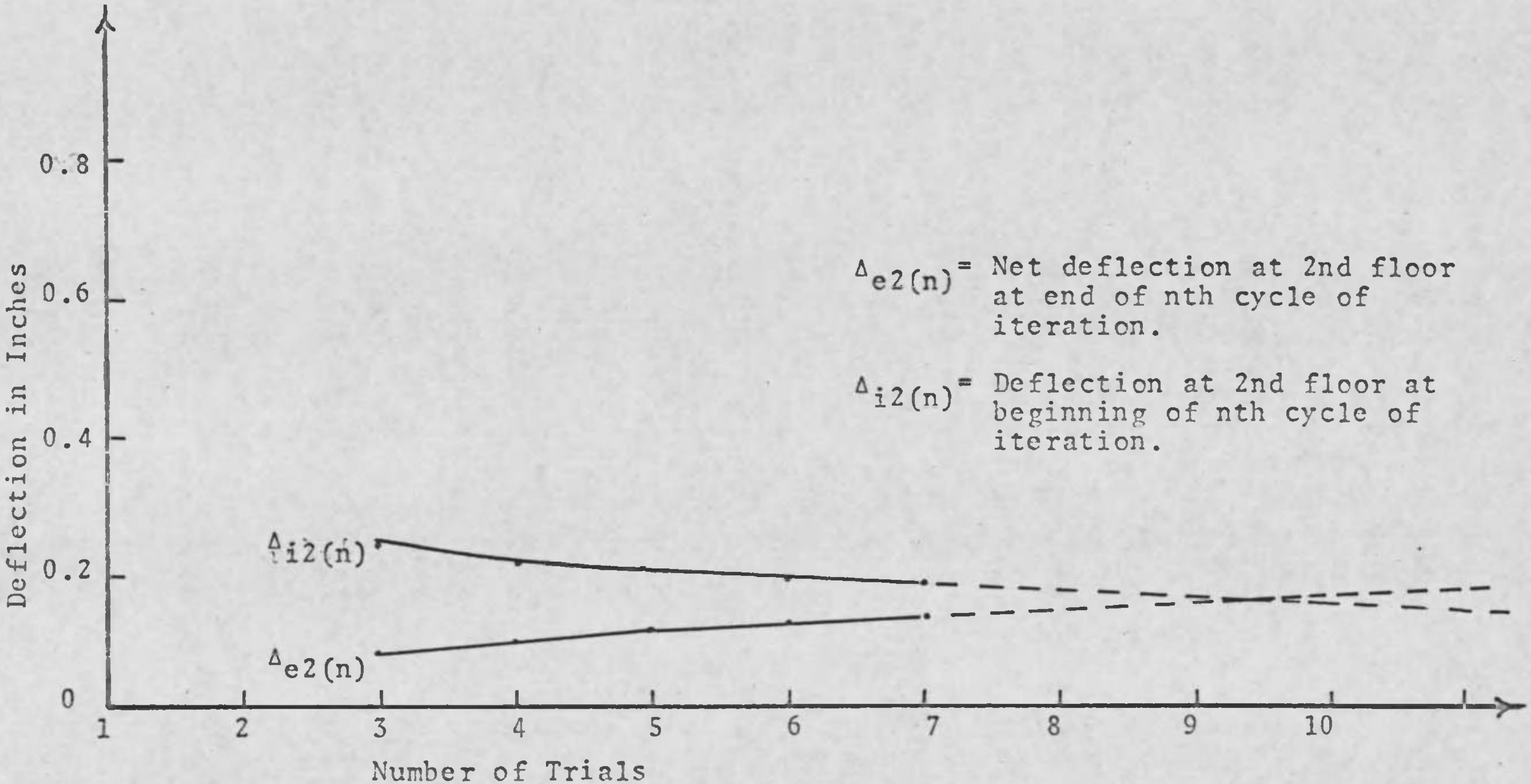

Figure 10. Rate of Convergence of Deflections at Second Floor.

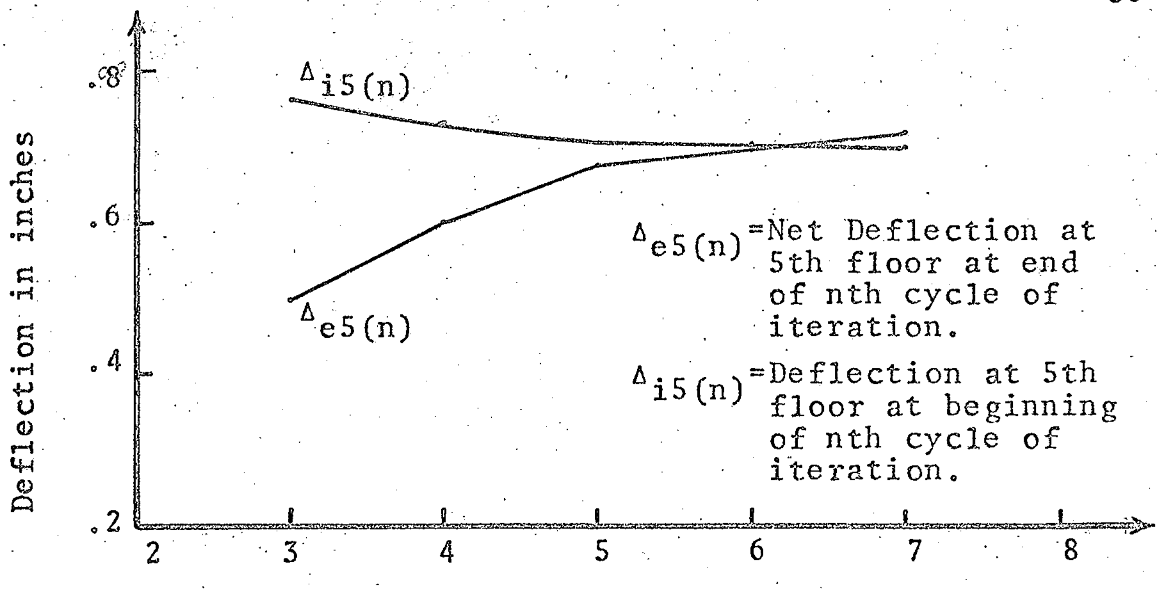

Figure 11. Rate of Convergence of Deflections at 5th Floor.

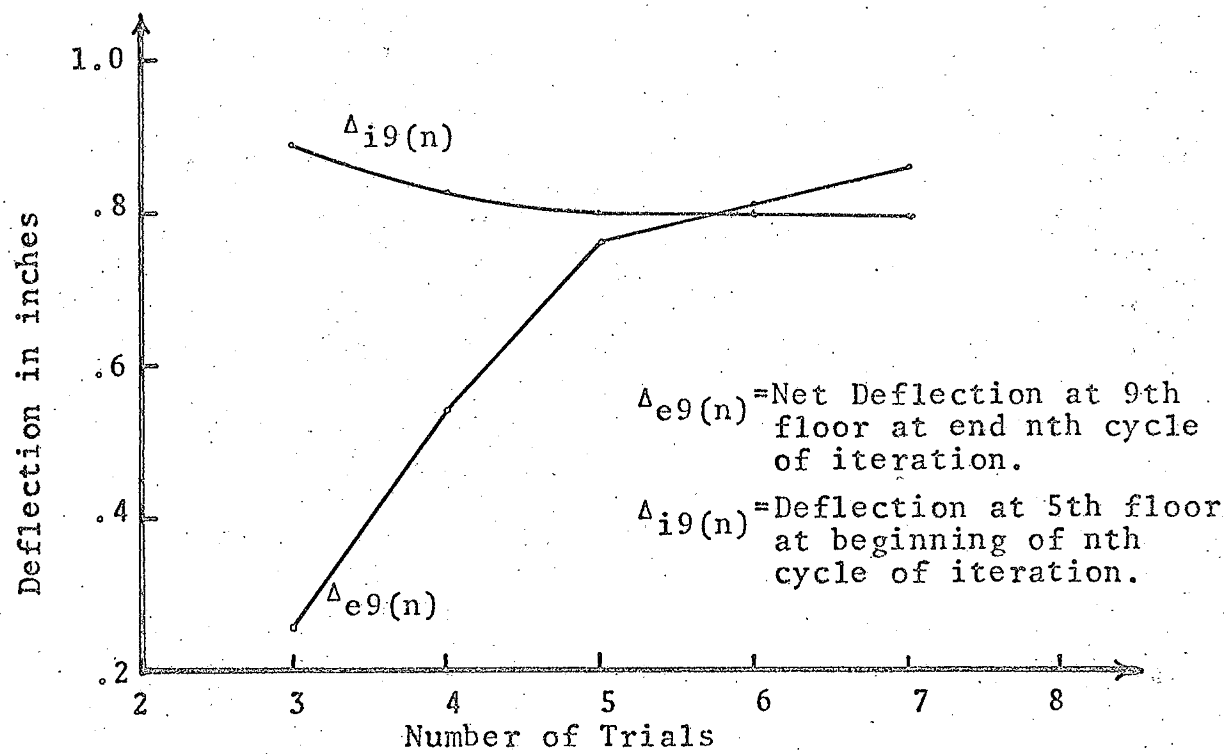

Figure 12. Rate of Convergence of Deflections at 9th Floor.

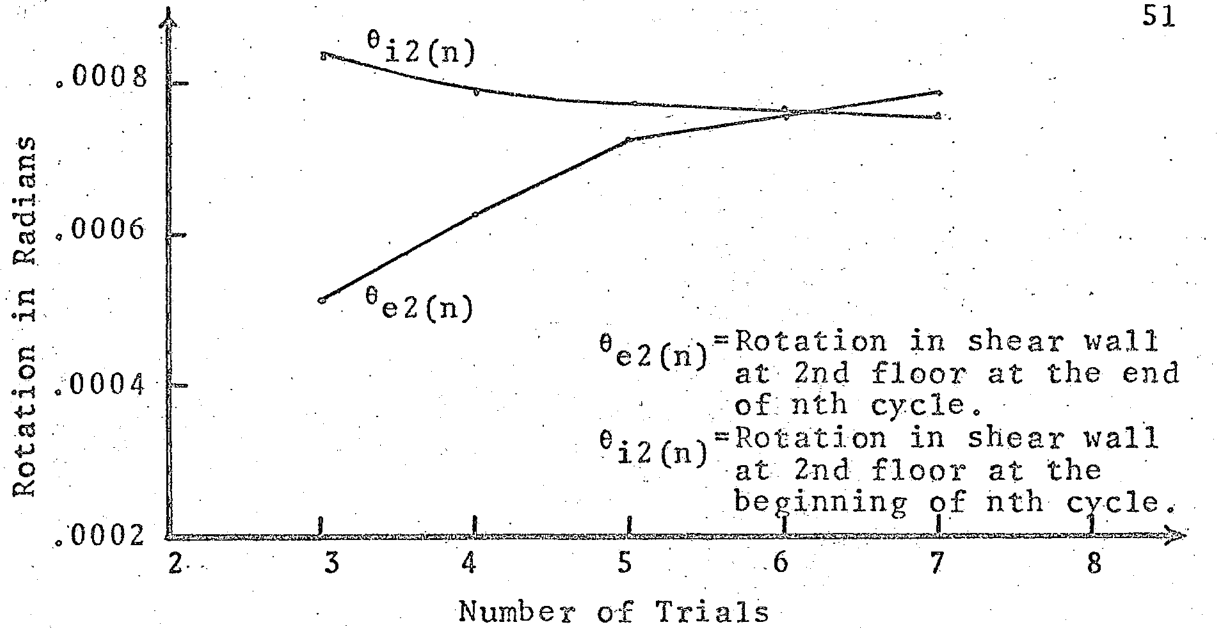

Figure 13. Rate of Convergence of Rotations at 2nd Floor.

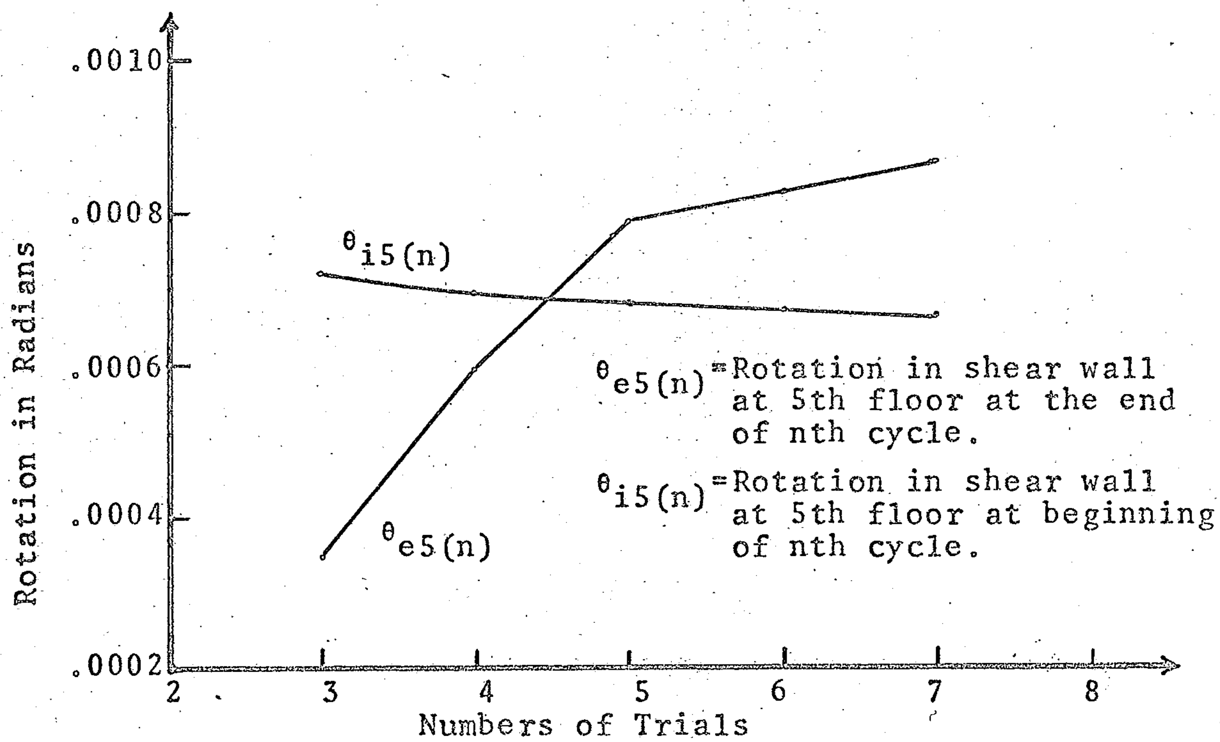

Figure 14. Rate of Convergence of Rotations at 5th Floor.

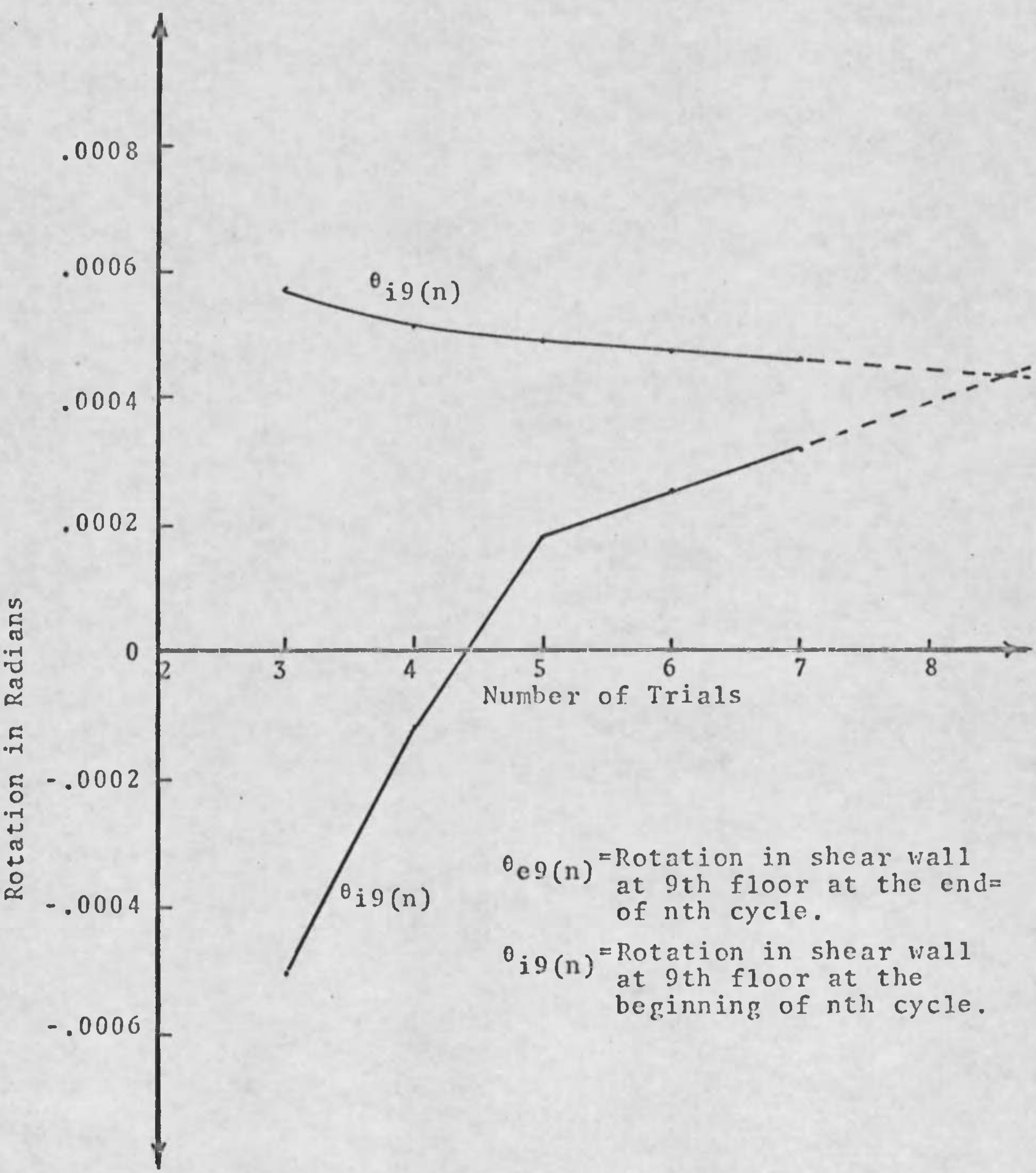

Figure 15. Rate of Convergence of Rotations at 9th Floor.

Wall-column stiffness ratio, $\frac{S_s}{S_c}=96$

Column-Beam stiffness ratio, $\frac{S_c}{S_B}=4$

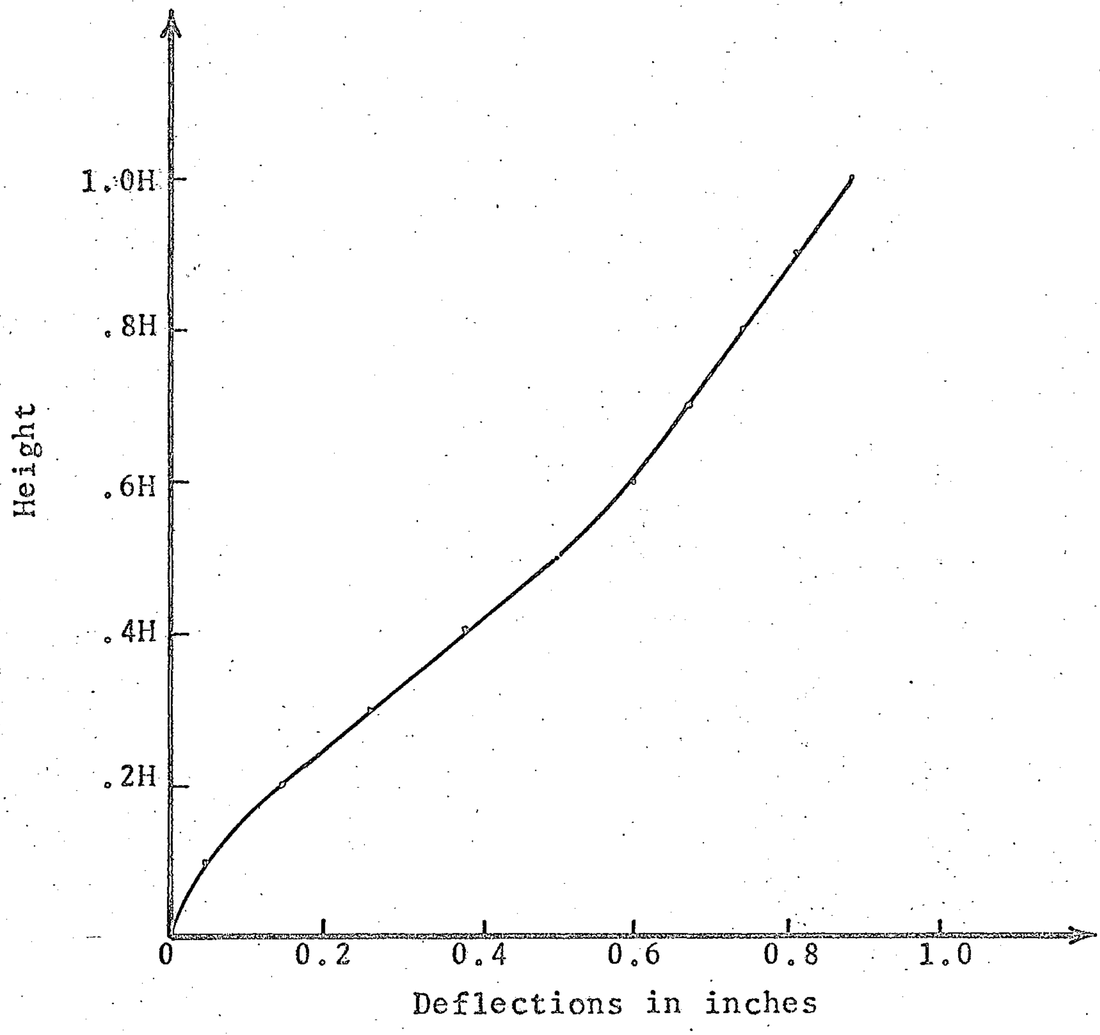

Figure 16. Deflection vs. Height (with base rotation).

<u>Derivation of Algebraic Equation.</u>

The deflections versus story height graph (Fig. 16) is plotted and the algebraic equation for the graph is derived as follows:

The general equation for curve is

$$y = Ax^n + Bx + C$$

But $x = 0$, $y = 0$ $\quad C = 0$

$\therefore y = Ax^n + Bx$ $\qquad$ conditions from graph

$x = 0.6$	$y = 0.6$
$x = 0.36$	$y = 0.33$
$x = 0.216$	$y = 0.16$

$$\therefore 0.6 = A(0.6)^n + 0.6B$$

$$0.33 = A(0.36)^n + 0.36B$$

$$0.33 = A(0.6)^{2n} + 0.36B$$

$$\underline{0.36 = 6A(0.6)^n + 0.36(B)}$$

$$-.03 = A(0.6)^{2n} - 6A(0.6)^n$$

$$\therefore A = \frac{.03}{0.6(0.6)^n - (0.6)^{2n}}$$

and

$$0.6 = A(0.6)^n + 0.6B$$

$$0.16 = A(.216)^n + 216B$$

$$0.16 = A(0.6)^{3n} + .216B$$

$$\underline{.216 = .36A(.6)^n + .216B}$$

$$-.056 = A[.6^{3n} - .36(.6)^n]$$

$$\therefore A = \frac{.056}{.36(.6)^n - (.6)^{3n}}$$

$$\therefore \frac{.03}{.6(.6)^n - (.6)^{2n}} = \frac{.056}{.36(.6)^n - (.6)^{3n}}$$

$$\therefore \frac{.36(.6)^n-(.6)^{3n}}{.6(.6)^n-(.6)^{2n}} = \frac{.056}{.03} = 1.865$$

$$\therefore 0.36(.6)^n-(.6)^{3n}=1.12(.6)^n-1.865(.6)^{2n}$$

$$\therefore 0.36-0.6^{2n}=1.12-1.865(0.6)^n$$

$$\therefore 0.6^{2n}-1.865(.6)^n-.76=0$$

$$0.6^n= \frac{+1.865\pm\ 3.48-3.04}{2}$$

$$= \frac{1.865\pm.632}{2}$$

$$=1.248 \text{ or } 0.616$$

$$\therefore n \log.6= \log 1.248 \text{ or } \log 0.616$$

$$n=\frac{0.096}{\bar{1}.778} \quad \text{or} \quad \frac{\bar{1}.79}{\bar{1}.778}$$

$$=\frac{+0.096}{-\ .222} \quad \text{or} \quad \frac{-0.21}{-0.222}$$

$$=-0.432 \quad \text{or} \quad 0.95$$

Now $$A=\frac{.03}{0.6(0.6)^n-(0.6)^{2n}}$$

substituting values of "n" in above equation

$n=-0.432$ $\qquad$ $A=-0.037$

and

$n=0.95 \qquad A=-3.00$

$$B=\frac{-A(0.6)^{n}+0.6}{0.6}$$

$n=-0.432$ and $A=-.037 \qquad B=1.076$

$n=0.95$ and $A=-3.0 \qquad B=4.08$

$$\therefore\ y=-.037x^{-.432}+1.076x=1.076x-\frac{0.037}{x^{0.432}}$$

or

$$y=-3x^{0.45}+4.08x=4.08x-3x^{0.95}.$$

From Khan's charts (1) (Fig. 32 through Fig. 38), it is clear that the variation of column-beam stiffness ratio, $\frac{S_c}{S_B}$ does not radically affect the graph. But wall-column stiffness ratio, $\frac{S_s}{S_c}$ has seemingly important influence. So for constant value of $\frac{S_s}{S_c}$ (i.e. 96), our derived algebraic equations give the deflected shape close to the final deflected shape regardless of the value of $\frac{S_s}{S_B}$ ratio.

CHAPTER 5

CONCLUSIONS

A practical method of analysis for the multistory framed structure with moment-resisting joints that is also braced with shear walls has been proposed in this thesis. The method does not require simplifying assumptions that are not ultimately checked and yet gives the designer some freedoms as follows:

1. Variable story heights are permitted.
2. Constant shear walls are not needed and the openings in shear walls are allowable.
3. Variable sections of columns and girders are allowed.

The common design assumptions that all horizontal loads are carried by the shear walls are not correct over the entire height of the structure. Furthermore the distribution of the lateral shear between the frame and the shear wall depends not only on their relative stiffnesses but on the number of stories as well.

The iterative procedure adapted in this thesis is laborious and requires time and patience. In spite of that, the procedure is simple and a problem can be solved on a sliderule or a small desk calculator in the design offices.

The concept of the substitute cantilever for the frame reduces the multibayed structure into the single bay structure. A numerical example is presented to illustrate the design procedure and simplicity of the calculations. For the final trial of the example, the moment distributions involved in both the proposed and basic methods are presented in Appendix I(B) in order to show that a considerable amount of work is saved by the proposed moment distribution.

The use of Khan's Charts (1) to get the approximated final deflected shape of the frame is recommended in order to obtain faster convergence of the iteration.

The method presented is easily applicable to the design of the shear wall buildings of any height for maximum economy with adequate control over the required strength and ductility of all structural elements.

Base rotation is considered in Chapter 4 and results both, with and without base rotations, are tabulated in Table 5 for comparison purposes. The overall difference for horizontal shear and bending moment is within four percent for this example building in both cases with and without base rotation. The maximum difference in the deflection is also four percent. Thus, it seems that the base rotation has insignificant influence in the iterative analysis for at least some building proportions.

The same numerical example is solved again in Chapter 4 with inclusion of the base rotation and without use of Khan's charts to obtain an approximate close deflected shape to start with. It is seen that the example without use of charts requires three more trials than that with use of charts. Therefore, if the charts are not available, the graphs can be plotted for first six or seven iterative trials starting from free deflected shape with or without base rotation. Then the intersection values which are correct or quite close to correct values can be read directly if the graphs intersect otherwise extend to let them intersect.

The algebraic equation that is derived from deflection versus height graph is restricted to concentrated loading and to wall-column stiffness ratio of about 100.

APPENDIX I(A)

Free Deflections and Rotations; Shear Wall.

Story	External Load K	Story Shear K	Bend. Mom. K'
10	12	12	0
9	22	34	-144
8	26	60	-552
7	24	84	-1272
6	24	108	-2280
5	24	132	-3576
4	24	156	-5160
3	24	180	-7032
2	24	204	-9192
1	24	228	-11640
Ground	12	240	-14376

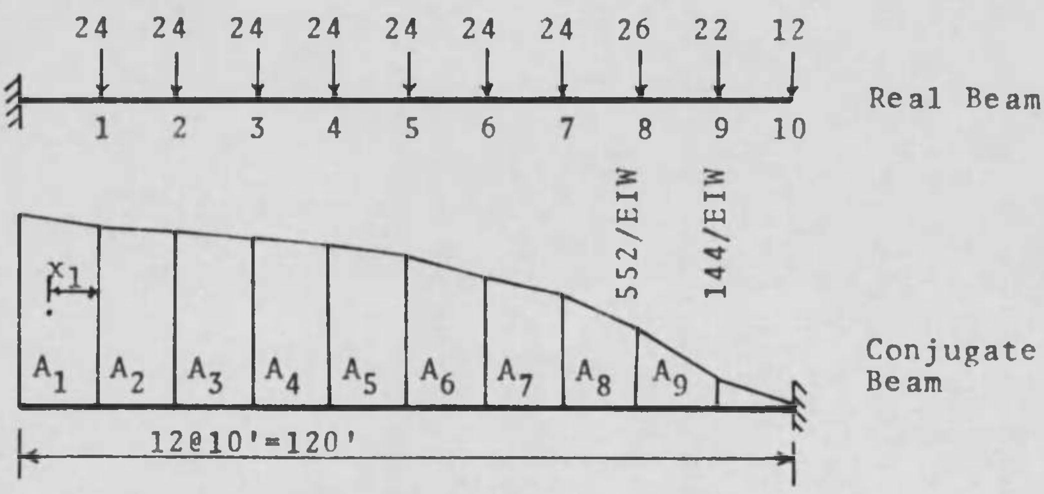

$$\text{Area } A_1 = \frac{14376+11640}{2\ EIw} \times 12$$

$$\therefore EI_w A_1 = 156{,}096 \text{ K.Ft}^2.$$

Similarly,

$EIA_2 = 124992$

$EI_w A_3 = 97{,}344$

$EI_w A_4 = 73{,}152$

$EI_w A_5 = 52{,}416$

$EI_w A_6 = 35{,}136$

$EI_w A_7 = 21{,}312$

$EI_w A_8 = 10{,}944$

$EI_w A_9 = 4{,}176$

$EI_w A_{10} = 864$

$$x_1 = \frac{11640+2(14376)}{11640+14376} \times \frac{12}{3}$$

$$= \frac{40392}{26016} \times 4$$

$$= 6.2 \text{ Ft.}$$

Similarly,

$x_2 = 6.23$ Ft.

$x_3 = 6.27$ Ft.

$x_4 = 6.31$

$x_5 = 6.37$

$x_6 = 6.32$

$x_7 = 6.57$

$x_8 = 6.78$

$x_9 = 7.15$

$x_{10} = 8.00$

Rotations.

$$\theta_{f_1} = A_1 = \frac{156{,}096}{EI_w}$$

$$= \frac{156{,}096}{(3420 \times 144)200}$$

$$= \frac{156{,}096}{9.85 \times 10^7}$$

$$= 0.00158 \text{ Radians}$$

$$\theta_{f_2} = A_1 + A_2$$

$$= \frac{156{,}096 + 124{,}992}{9.85 \times 10^7}$$

$$= 0.00285 \text{ Rad.}$$

$$\theta_{f_3} = A_1 + A_2 + A_3$$

$$= 0.0036$$

Similarly,

$\theta_{f_4}=0.0044$ Rad.

$\theta_{f_5}=0.00493$

$\theta_{f_6}=0.00527$

$\theta_{f_7}=0.0055$

$\theta_{f_8}=0.0056$

$\theta_{f_9}=0.00565$

$\theta_{f_{10}}=0.00566$

<u>Deflections</u>.

$$\Delta_{f1}=A_1x_1$$

$$=\frac{156{,}096\times 6.2}{(3420\times 144)\ 200}\times 12$$

$$=\frac{156{,}096\times 6.2}{8.208\times 10^6}$$

$$=0.128$$

$$=0.13 \text{ in.}$$

$$\Delta_{f_2}=A_1(12+x)+A_2x_2$$

$$=\frac{156{,}096(18.2)+124{,}992(6.23)}{8.208\times 10^6}$$

$$=0.46 \text{ in.}$$

$$\Delta_{f_3} = A_1(24+x_1) + A_2(12+x_2) + A_3x_3$$

$$= 0.96 \text{ in.}$$

Similarly,

$\Delta_{f_4} = 1.57$

$\Delta_{f_5} = 2.28$

$\Delta_{f_6} = 3.05$

$\Delta_{f_7} = 3.86$

$\Delta_{f_8} = 4.69$

$\Delta_{f_9} = 5.53$

$\Delta_{f_{10}} = 6.37$

APPENDIX I(B)

Moment Distributions.

1. Proposed method - First Trial
2. Proposed Method - Final Trial
3. Basic Method - Final Trial

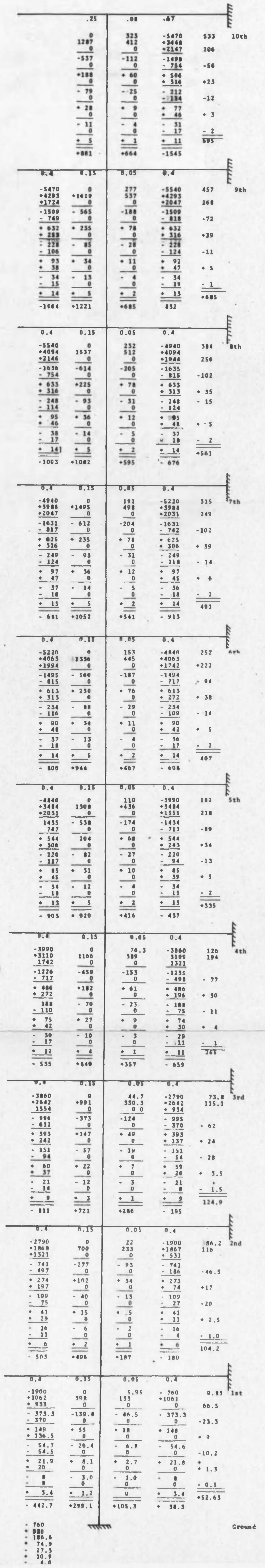

10th
9th
8th
7th
6th
5th
4th
3rd
2nd
1st
Ground

Final Trial Proposed Method

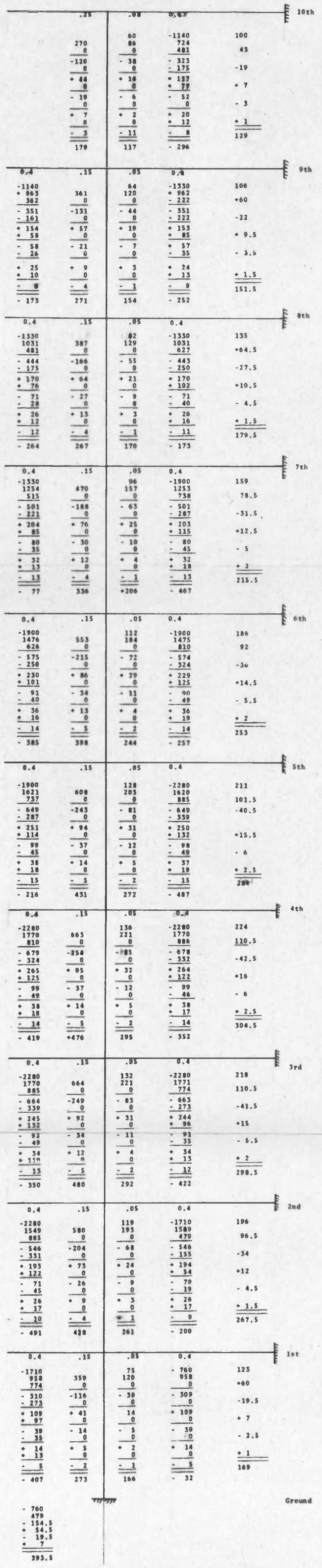

Final Trial - Basic Method

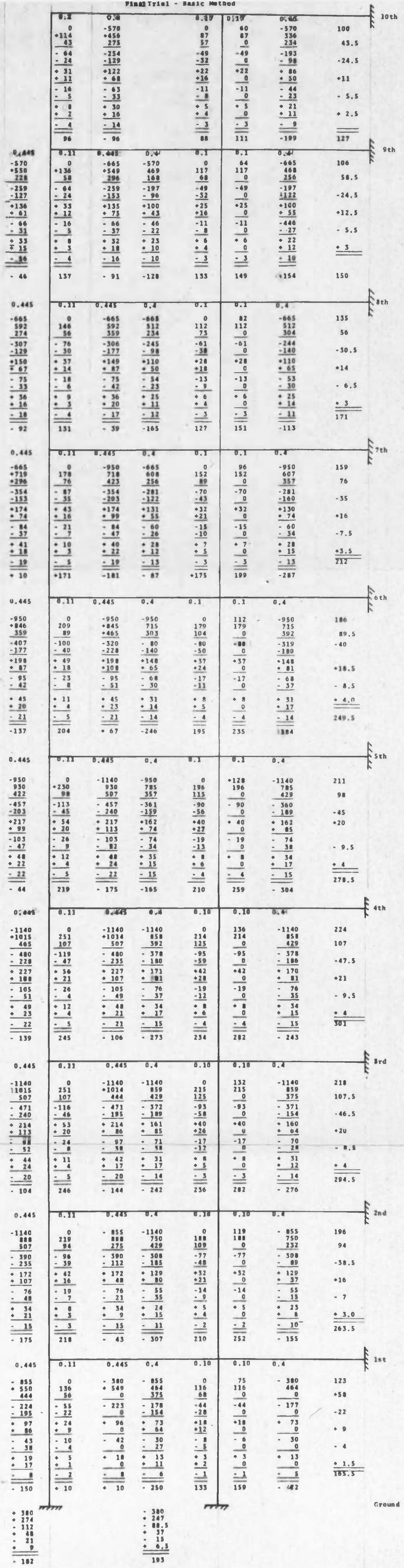

APPENDIX I(C)

Tabulated results of the deformations of the wall from 1 through 6 trials.

Table 6. Deflection and Rotation for First Cycle.

Story	Deflection: Free Δ_{fi} in.	Initial $\Delta_{ii(1)}$ in.	Net $\Delta_{ei(1)}$ in.	Initial for next cycle $\Delta_{ii(2)}$ in.	Rotations: Free θ_{fi} Rad.	Initial $\theta_{ii(1)}$ Rad	Net $\theta_{ei(1)}$ Rad	Initial for next cycle $\theta_{ii(2)}$ Rad.
10	6.37	2.07	-7.14	0.85	.00566	.00184	-.009	0.00064
9	5.53	1.782	-5.61	0.76	.00565	.00158	-.00866	0.00055
8	4.69	1.49	-5.21	0.61	.0056	.001325	-.00802	0.000495
7	3.86	1.23	-3.32	0.564	.0055	.00109	-.00714	0.00043
6	3.05	0.955	-2.36	0.46	.00527	.00087	-.0061	0.00037
5	2.28	0.70	-1.57	0.35	.00493	.00063	-.00495	0.0003
4	1.57	0.49	-0.94	0.256	.0044	.000436	-.00375	0.000224
3	0.96	0.287	-0.49	0.16	.00364	.000255	-.00259	0.000135
2	0.46	0.14	-0.195	0.081	.00285	.000125	-.00152	0.000078
1	0.13	0.04	-0.0425	0.0245	.00158	.000034	-.00063	0.000028

Table 7. Deflection and Rotation for Second Cycle.

Story	Deflections: Free Δ_{fi} in.	Deflections: Initial $\Delta_{ii(2)}$ in.	Deflections: Net $\Delta_{ei(2)}$ in.	Deflections: Initial for next cycle $\Delta_{ii(3)}$ in.	Rotations: Free θ_{fi} Rad.	Rotations: Initial $\theta_{ii(2)}$ Rad.	Rotations: Net $\theta_{ei(2)}$ Rad.	Rotations: Initial for next cycle $\theta_{ii(3)}$ Rad.
10	6.37	0.85	1.31	0.92	.00566	.00064	.000414	.000615
9	5.53	0.76	1.26	0.835	.00565	.00055	.000475	.000543
8	4.69	0.61	1.175	0.6937	.0056	.000495	.000675	.0005114
7	3.86	0.564	1.06	0.647	.0055	.00043	.000905	.0004706
6	3.05	0.46	0.92	0.542	.00527	.00037	.00108	.0004277
5	2.28	0.35	0.75	0.4245	.00493	.0003	.00126	.000373
4	1.57	0.256	0.56	0.3175	.0044	.000224	.00135	.000301
3	0.96	0.16	0.367	0.204	.00364	.000135	.00131	.0001995
2	0.46	0.081	0.19	0.106	.00284	.000078	.00112	.000123
1	0.13	0.0245	0.054	0.0317	.00158	.000028	.0007	.000362

Table 8. Deflection and Rotation for Third Cycle.

	Deflections				Rotations			
Story	Free Δ_{fi} in.	Initial $\Delta_{ii(3)}$ in.	Net $\Delta_{ei(3)}$ in.	Initial for next cycle $\Delta_{ii(4)}$ in.	Free θ_{fi} Rad.	Initial $\theta_{ii(3)}$ Rad.	Net $\theta_{ei(2)}$ Rad.	Initial for next cycle $\theta_{ii(4)}$ Rad.
10	6.37	0.92	0.99	0.9302	.00566	.00064	.0001192	.000656
9	5.53	0.835	0.97	0.856	.00565	.00055	.000185	.000511
8	4.69	0.6937	0.92	0.729	.0056	.000495	.00039	.0005006
7	3.86	0.647	0.86	0.685	.0055	.00043	.000621	.000484
6	3.05	0.542	0.753	0.581	.00527	.00037	.00081	.0004613
5	2.28	0.4245	0.625	0.4655	.00493	.0003	.00099	.0004267
4	1.57	0.3175	0.471	0.3517	.0044	.000224	.00109	.0003665
3	0.96	0.204	0.314	0.2306	.00364	.000135	.0011	0.0002653
2	0.46	0.106	0.1625	0.1223	.00284	.000078	.000955	0.0001737
1	0.13	0.0317	0.0317	0.0361	.00158	.000028	.00061	0.0000568

Table 9. Deflections and Rotations for Fourth Cycle.

Story	Deflections: Free Δ_{fi} in.	Initial $\Delta_{ii(4)}$ in.	Net $\Delta_{ei(4)}$ in.	Initial for next cycle $\Delta_{ii(5)}$ in.	Rotations: Free θ_{fi} Rad.	Initial $\theta_{ii(4)}$ Rad.	Net $\theta_{ei(4)}$ Rad.	Initial for next cycle $\theta_{ii(5)}$ Rad.
10	6.37	0.9302	0.905	0.92	.00566	.000565	.00058	.0003181
9	5.53	0.856	0.884	0.87	.00565	.000511	.000845	.000504
8	4.69	0.729	0.846	0.79	.0056	.0005006	.000977	.0006211
7	3.86	0.685	0.775	0.73	.0055	.000484	.00098	.000673
6	3.05	0.581	0.678	0.63	.00527	.0004613	.000887	.000657
5	2.28	0.4655	0.57	0.52	.00493	.0004267	.00073	.000596
4	1.57	0.3517	0.428	0.39	.0044	.0003665	.000576	.000480
3	0.96	0.2306	0.297	0.26	.00364	.0002653	.000375	.000438
2	0.46	0.1223	0.154	0.14	.00284	.0001737	.000197	.000354
1	0.13	0.0361	0.045	0.04	.00158	.0000568	.000139	.000352

Table 10. Deflection and Rotation for Fifth Cycle.

Story	Deflections				Rotations			
	Free Δ_{fi} in.	Initial $\Delta_{ii(5)}$ in.	Net $\Delta_{ei(5)}$ in.	Initial for next cycle $\Delta_{ii(6)}$ in.	Free θ_{fi} Rad.	Initial $\theta_{ii(5)}$ Rad.	Net $\theta_{ei(5)}$ Rad.	Initial for next cycle $\theta_{ii(6)}$ Rad.
10	6.37	0.92	1.03	0.939	0.00566	.0003181	.00059	.000367
9	5.53	0.87	0.956	0.884	0.00565	.000509	.000636	.000364
8	4.69	0179	0.874	0.804	0.0056	.0006211	.000755	.000464
7	3.86	0.73	0.78	0.74	0.0055	.000673	.000886	.000518
6	3.05	0.63	0.665	0.637	0.00527	.000657	.00083	.000617
5	2.28	0.52	0.538	0.524	0.00493	.000596	.000912	.000693
4	1.57	0.39	0.403	0.393	0.0044	.000480	.000952	.000718
3	0.96	0.26	0.267	0.262	0.00364	.000438	.000938	.000680
2	0.46	0.14	0.14	0.14	0.00284	.000354	.00081	.000629
1	0.13	0.04	0.04	0.04	0.00158	.000352	.000524	.000366

Table 11. Deflection and Rotation For Sixth Cycle.

Story	Free Δ_{fi} in.	Initial $\Delta_{ii(6)}$ in.	Net $\Delta_{ei(6)}$ in.	Initial for next cycle $\Delta_{ii(7)}$ in.	Free θ_{fi} Rad.	Initial $\theta_{ii(6)}$ Rad.	Net $\theta_{ei(6)}$ Rad.	Initial for next cycle $\theta_{ii(7)}$ Rad.
10	6.37	0.939	0.87	0.89	.00566	.000367	.000484	.000425
9	5.53	0.884	0.79	0.83	.00565	.000364	.000732	.000680
8	4.69	0.804	0.75	0.76	.0056	.000464	.00083	.000755
7	3.86	0.74	0.65	0.69	.0055	.000518	.00083	.000774
6	3.05	0.637	0.55	0.59	.00527	.000617	.000765	.000729
5	2.28	0.52	0.47	0.49	.00493	.000693	.00067	.000643
4	1.57	0.393	0.35	0.37	.0044	.000718	.000582	.000550
3	0.96	0.26	0.25	0.25	.00364	.000680	.000473	.000468
2	0.46	0.14	0.13	0.13	.00284	.000629	.000373	.000368
1	0.13	0.04	0.04	0.04	.00158	.000366	.000367	.000347

APPENDIX II

NOTATIONS

D = The dimension of the building in feet in a direction parallel to the applied forces.

D_n = Relative displacement of the two ends of member n.

d_n^f = $2E\theta_n^f$ = Deformation at joint n.

E = Modulus of elasticity

FM_{ci} = Fixed end moment of column at ith story.

FM_{biw} = Fixed end moment of linkbeam at ith story at its wall end.

FM_{bif} = Fixed end moment of linkbeam at ith story at its frame end.

F_i = Lateral forces applied to a level designated as "i".

h_n = Height of nth story.

h_i = Height in feet above the base to the level designated as "i".

I_f = Moment of inertia of wall footing.

I_w = Moment of inertia of shear wall.

J = Numerical coefficient for base moment as specified in Chapter 4.

k = Subgrade soil modulus in pounds per square inch per inch of deformation.

K_n^c = Σk_n^c = The sum of all column stiffnesses at nth story.

K_n^{lb} = Σk_n^{lb} = The sum of all linkbeam stiffnesses at nth story.

k_n^c = Stiffness of column between floor n and n-1.

k_n^b = Stiffness of beam at nth floor.

k_n^{lb} = Stiffness of linkbeam at nth floor.

ℓ_n^w = Half the width of shear wall at nth floor.

M_{AB} = Resultant end moment at point A of member AB

M_{AB}^F = Fixed end moment at point A of member AB

M_b = Overturning moment at the base of the shear wall.

M_i' = Concentrated moment on shear wall at floor i.

M_i = Applied moment on shear wall by linkbeam at floor i.

P_i = External load at floor i.

R_{vi} = Vertical reaction of the link beam at the shear wall at floor i.

T = Fundamental period of vibration of the structure in seconds.

θ_n^f = Joint rotation of framework at nth floor.

θ_n^w = Rotation of shear wall at nth floor.

θf_i = Free rotation of wall at floor i.

$\theta_{ii(n)}$ = Rotation in shear wall at ith floor at the beginning of nth cycle.

$\theta_{ei(n)}$ = Rotation in shear wall at ith floor at the end of nth cycle.

Δ_{fi} = Free deflection of wall at floor i.

$\Delta_{ii(n)}$ = Deflection at ith floor at beginning of nth cycle of iteration.

$\Delta_{ei(n)}$ = Net deflection at ith floor at end of nth cycle of iteration.

REFERENCES

1. Khan, Fazlur R., John A. Sbarounis, "Interaction of Shear Walls and Frames." Journal of A.S.C.E. Vol. 90 ST3, p. 285.

2. Tamhankar, M. G., J. P. Jain, G. S. Ramaswamy, "The Concept of Twin Cantilevers in the Analysis of Shear-Walled Multistorey Buildings." Indian Conc. Journal p. 488 Dec. 1966.

3. Gould, Phillip L., "Interaction of Shear Wall-Frame Systems in Multistory Buildings." Journal of Am. Conc. Inst. p. 45, Jan. 1965.

4. Cardan, Bernhard, "Concrete Shear Walls Combined With Rigid Frames in Multistory Buildings Subject to Lateral Loads." Journal of Am. Conc. Inst. p. 299 Sept. 1961.

5. Thadani, B. N., "Analysis of Shear Wall Structures." Indian Conc. Journ. p. 97, March 1966.

6. "Building Code Requirements for Reinforced Concrete," Amer. Concrete Inst. Detroit, Mich., ACI 318-63, 1963.

7. Blume, John A., Nathan M. Newmark and Leo H. Corning, "Design of Multistory Reinforced Concrete Buildings for Earthquake Motions," Portland Cement Ass'n., Chicago, Ill., 1961.

8. Kinney, J. S., "Indeterminate Structural Analysis," Addison - Wesley Publishing Co., Inc. Reading, Massachusetts, 1957.

9. Sexton, H. J., Discussion of "Concrete Shear Walls Combined with Rigid Frames in Multistory Buildings Subject to Lateral Loads," by Bernard Cardan, Journ. of the Amer. Conc. Inst., part 2, Vol. 58, March, 1962, pp. 825-827.

10. Teng, Wayne C., "Foundation Design", Prentice-Hall, Inc. New Jersey, 1962, pp. 137-145.